

RPSEA

Final Report

***Treatment and Beneficial Reuse of
Produced Waters Using a Novel
Pervaporation-Based Irrigation
Technology***

09123.11.Final

March 16, 2014

Dr. Jonathan Brant
Department of Civil and Architectural Engineering
University of Wyoming
1000 University Avenue, Dept. 3295
Laramie, WY 82071

DISCLAIMER STATEMENT

LEGAL NOTICE

This report was prepared by **(Dr. Jonathan Brant)** as an account of work sponsored by the Research Partnership to Secure Energy for America, RPSEA. Neither RPSEA members of RPSEA, the National Energy Technology Laboratory, the U.S. Department of Energy, nor any person acting on behalf of any of the entities:

- a. **MAKES ANY WARRANTY OR REPRESENTATION, EXPRESS OR IMPLIED WITH RESPECT TO ACCURACY, COMPLETENESS, OR USEFULNESS OF THE INFORMATION CONTAINED IN THIS DOCUMENT, OR THAT THE USE OF ANY INFORMATION, APPARATUS, METHOD, OR PROCESS DISCLOSED IN THIS DOCUMENT MAY NOT INFRINGE PRIVATELY OWNED RIGHTS, OR**
- b. **ASSUMES ANY LIABILITY WITH RESPECT TO THE USE OF, OR FOR ANY AND ALL DAMAGES RESULTING FROM THE USE OF, ANY INFORMATION, APPARATUS, METHOD, OR PROCESS DISCLOSED IN THIS DOCUMENT.**

THIS IS A FINAL REPORT. THE DATA, CALCULATIONS, INFORMATION, CONCLUSIONS, AND/OR RECOMMENDATIONS REPORTED HEREIN ARE THE PROPERTY OF THE U.S. DEPARTMENT OF ENERGY.

REFERENCE TO TRADE NAMES OR SPECIFIC COMMERCIAL PRODUCTS, COMMODITIES, OR SERVICES IN THIS REPORT DOES NOT REPRESENT OR CONSTITUTE AND ENDORSEMENT, RECOMMENDATION, OR FAVORING BY RPSEA OR ITS CONTRACTORS OF THE SPECIFIC COMMERCIAL PRODUCT, COMMODITY, OR SERVICE.

THIS PAGE INTENTIONALLY LEFT BLANK

ABSTRACT

Pervaporation is a non-pressure driven membrane process that may facilitate desalination of saline waters with less energy and pretreatment requirements relative to conventional desalination processes. This study investigated combining this technology with subsurface drip irrigation, in a process termed subsurface pervaporation irrigation, as a means for small producers to manage produced waters associated with oil and natural gas development. Small producers were targeted for this technology given the characteristically lower generation rates of produced water that is associated with this group. Non-porous, hydrophilic membranes were evaluated for use in the pervaporation irrigation application. Flat-sheet and corrugated tubular membrane configurations were studied to establish performance specifications for the system treating model and actual produced water samples. Process performance was evaluated in terms of water flux and salt rejection, as well as in terms of impacts on the soil quality and vegetation growth. Membrane performance was determined to be a function of the membrane properties (thickness, affinity for water) and operating conditions (vapor pressure gradient across the membrane, feed water salinity, evapotranspiration, composition of the surrounding medium). Water flux ranged from 0.2 to 974 liters per square meter per hour (LMH) for the different pervaporation membranes studied and application scenarios. Independent of the membrane properties, produced water chemistry/composition, or application was the measured salt rejection, which was consistently $\geq 95\%$. Water fluxes remained stable even as the feed water salinity increased over time indicating potential for long-term use as an irrigation system.

TABLE OF CONTENTS

| | |
|---|-----------|
| <i>DISCLAIMER STATEMENT</i> | 2 |
| <i>ABSTRACT</i> | 4 |
| <i>TABLE OF CONTENTS</i> | 5 |
| <i>LIST OF TABLES</i> | 7 |
| <i>LIST OF FIGURES</i> | 8 |
| <i>EXECUTIVE SUMMARY</i> | 10 |
| <i>INTRODUCTION</i> | 13 |
| Objectives | 13 |
| <i>BACKGROUND</i> | 14 |
| Oil and Natural Gas Produced Waters | 14 |
| Treatment Methods for Produced Waters | 15 |
| Beneficial Reuse | 16 |
| Pervaporation | 17 |
| Pervaporation Irrigation system | 18 |
| <i>EXPERIMENTAL METHODS</i> | 20 |
| Membranes | 20 |
| Membrane Surface Chemistry - <i>Contact Angle Measurements</i> | 21 |
| Water Uptake by Pervaporation Membranes - <i>Swelling Analysis</i> | 22 |
| Pervaporation Membrane Surface Morphology - <i>Scanning Electron Microscopy (SEM)</i> | 22 |
| Bench-Scale Pervaporation Experiments | 23 |
| Bench-Scale Soil Box Experiments | 28 |
| Bench Scale Grow Box Experiments | 30 |

| | |
|---|-----------|
| Field Trials | 31 |
| Coalbed Methane (CBM) and Conventional Produced Source Waters | 33 |
| <i>RESULTS AND DISCUSSION</i> | 36 |
| Membrane Surface Chemistry | 36 |
| Membrane Affinity for Water | 36 |
| Physical Characteristics and Elemental Composition of the CTA and PEE Membranes | 38 |
| Bench-Scale Pervaporation performance Testing | 41 |
| Relationships between Water Flux, Water Temperature, and Membrane Thickness | 41 |
| Effects of solutes on the Pervaporation Membrane Performance (Flux and Rejection) | 44 |
| performance assessment of pervaporation irrigation | 50 |
| Soil box experiments – Effect of membrane characteristics, environmental conditions on the membrane performance | 50 |
| Grow box assessment of pervaporation irrigation performance | 59 |
| Practical Aspects of Pervaporation Irrigation | 65 |
| Impact to Small Producers | 67 |
| Technology Transfer Efforts | 67 |
| <i>CONCLUSIONS</i> | 69 |
| <i>RECOMMENDATIONS</i> | 71 |
| <i>REFERENCES</i> | 72 |

LIST OF TABLES

| | |
|--|----|
| Table 1 - Summary of select disposal methods and treatment technologies typically used for managing produced waters. | 15 |
| Table 2 - Summary of select physical properties for the flat-sheet (second installment) and tubular forms of PEE and CTA membranes. | 21 |
| Table 3 - Summary of test conditions changed in each of the soil box bench scale experiments. Test conditions that were kept the same for each test include: airflow through soil box (1 L min^{-1}), depth of soil (20 cm), volume of soil (0.25 m^3), and depth of tubing within the soil (10 cm). PEE membranes of different thicknesses were used for tests 1-8. A CTA membrane was used for test 9. Additionally the feed water was recycled through the membrane tubing for tests 8 and 9. | 29 |
| Table 4 - Select water quality measures for the CBM produced water from the Dutch Creek site in Sheridan, WY..... | 34 |
| Table 5 - Select water quality values for the two conventional produced water samples. All water quality measurements were done by the Wyoming Analytical Laboratory (WAL), with the exception of pH, conductivity and total dissolved solids analyses. | 35 |
| Table 6 - Summary of contact angle values for the water, formamide, and diiodomethane probe liquids on the CTA and flat-sheet PEE membranes ($T = 24^\circ\text{C}$, $\text{pH} = 5.5$, $I = 0.0 \text{ M}$; $n = 15$). ... | 37 |
| Table 7 - Fractional increase in mass due to water uptake for the pervaporation tubing at the end of 3 days in solutions with varying ionic strength. The data shown are the final measurements taken of the samples ($\text{pH of DDW} = 5.5$, $\text{pH of CBM water} = 7.9$, $T = 24^\circ\text{C}$, $n = 3$)..... | 38 |
| Table 9 - Summary of average water fluxes and environmental variables for the soil box tests. | 54 |

LIST OF FIGURES

| | |
|---|----|
| Figure 1 – Conceptual illustration of the pervaporation process involving a hydrophilic membrane..... | 18 |
| Figure 2 - Process flow diagram of the cross flow pervaporation test unit. Blue lines correspond to the liquid flow lines, green lines correspond to dry air flow lines and the red lines correspond to the air and water vapor flow lines..... | 27 |
| Figure 3 - Experimental set-up for the bench-scale pervaporation irrigation tests (soil box). | 30 |
| Figure 4 - Experimental set-up for the bench-scale pervaporation irrigation tests (grow box)... | 31 |
| Figure 5 – Diagram and layout of the test plots used at in the field trials of the pervaporation irrigation system..... | 32 |
| Figure 7 - Field scanning electron microscopy (FESEM) image of a virgin CTA membrane used in the pervaporation experiments. The CTA membrane has an active layer thickness of 10 μm (top arrow in image), with a porous/fibrous support layer beneath the active layer (bottom arrow). The total thickness of the CTA membrane was 115 μm . The scale bar in the image reads 50 μm | 41 |
| Figure 8 - Water flux as a function of the vapor pressure differential between the feed water and sweeping gas for each of the different thicknesses of the (a) flat-sheet PEE and (b) CTA membranes. The feed water used was DDW ($\text{pH} = 5.5$, $n = 3$). | 43 |
| Figure 10 - Water flux rate as a function of sodium chloride (NaCl) concentration for the (a) 20 and 250 μm thick PEE membranes and the (b) CTA membrane ($\text{pH} = 5.5$, $\Delta VP = 12,275 \text{ Pa}$, $n = 2$). | 48 |
| Figure 11 - Water flux through the flat-sheet PEE membrane in the presence and absence of feed spacers ($l = 20 \mu\text{m}$, low air flow = 0.075 m sec^{-1} , high air flow = 0.170 m sec^{-1} , $[\text{NaCl}] = 100 \text{ g L}^{-1}$, $\Delta VP = 12,275 \text{ Pa}$, $n = 2$). | 48 |
| Figure 12 - Water flux for (a) 20 μm thick PEE membrane and (b) CTA membrane when using produced waters as feed waters in the bench-scale pervaporation experiments ($\Delta VP = 12,275 \text{ Pa}$, $T = 50^\circ\text{C}$, RH of sweeping gas = 2%, $n = 2$). | 49 |
| Figure 13 - Specific flux for the tubular PEE membrane when treating CBM water in the soil box apparatus. Each plot displays water fluxes through the tubing when surrounded by different | |

| | |
|---|----|
| types of soil: tests 1 and 2 used washed silica sand (a); tests 3-6 used garden soil (b), and test 7 used clay loam soil (c). Environmental/membrane conditions for each test are summarized in Table 3. | 53 |
| Figure 14 - Specific flux for the tubular PEE (Tests 7 and 8) and CTA (Test 9) membranes when treating CBM produced water in the soil box test apparatus (soil = clay loam, PEE thickness = 650 μm). | 55 |
| Figure 15 - Average specific flux ($\text{m}^3 \text{m}^{-2} \text{day}^{-1} \text{Pa}^{-1}$) through the PEE pervaporation tubing when surrounded by different soil types: washed silica sand (blue column); garden soil (red column); and clay loam soil (green column). The feed water used for each test was CBM water; the membrane thickness used for each sample was 650 μm | 56 |
| Figure 16 - Average specific flux ($\text{m}^3 \text{m}^{-2} \text{day}^{-1} \text{Pa}^{-1}$) for each thickness of the tubular PEE membrane when treating CBM produced water (soil = garden soil). The 400 μm thick membrane (56 g m^{-1}) is represented by the blue column, the 500 μm thick membrane (70 g m^{-1}) is represented by the red column, and the 650 μm thick membrane (90 g m^{-1}) is represented by the green column. | 57 |
| Figure 18 - Theoretical (y-axis) vs actual (x-axis) conductivity (mS cm^{-1}) of the reject water within the tubular PEE membrane during soil box Test 7. | 59 |
| Figure 19 - Specific flux rate of produced water through tubular CTA membrane. In test 9 the tubular PEE membrane was surrounded by clay loam soil. Tests For the grow box test garden soil surrounded the CTA pervaporation tube. Environmental/membrane conditions for tests 7 through 9 are summarized in Table 3. | 60 |
| Figure 20 - Grow box snapshots. The snapshot at the top was taken at the beginning of the test (07/25/13) and the bottom picture was taken after approximately 140 days (12/16/13) after the start of the test. The plants which died were about 10 or more inches away from the center of the tube while the plants that were still alive at the end of test were inline or less than 5 inches away from the center of the PV tube. | 61 |
| Figure 22 - Water flux ($\text{kg/m}^2/\text{day}$), cumulative weekly precipitation (mm), and vapor pressure gradient for the tubular PEE membrane during field trials when treating CBM produced water. | 64 |

EXECUTIVE SUMMARY

Water that is co-generated during the exploration for and extraction of oil and natural gas resources is termed produced water. These waters can contain a myriad of organic and inorganic substances, with specific compositions being a function of the formation properties and well age. Total dissolved solids (TDS) concentrations in produced waters can range from several hundred to several hundreds of thousands of milligrams per liter. Beneficial reuse of produced waters requires that the TDS concentration, as well as that of other constituents, be reduced to levels that meet the requirements of the intended reuse application.

From a treatment perspective, the high TDS concentrations that characterize produced waters are particularly challenging. Many options exist for desalinating produced waters; however, many of these technologies are not feasible for small producers given the cost and complexity of these systems. Pervaporation is a non-pressure driven membrane process that may facilitate desalination of saline waters with less energy and pretreatment requirements relative to conventional desalination processes. In this work hydrophilic pervaporation membranes were integrated into subsurface irrigation systems (subsurface pervaporation irrigation) to assess its feasibility for disposing of produced waters while at the same time beneficially reusing it. The expected outcome from this effort was a low-tech approach that small producers may use for managing produced water flows.

Two types of hydrophilic pervaporation membranes were evaluated in this study. The first was a polyetherester (PEE) membrane while the second was constructed of cellulose triacetate (CTA). Flat-sheet and tubular membrane configurations were studied to establish the performance specifications as a function of different environmental variables. Membrane performance, measured in terms of water flux and salt rejection, was dependent on the properties of the membrane and the surrounding environmental conditions. Water flux was inversely proportional to the thickness of the membrane's active layer. Water flux was higher for the CTA membrane, relative to that for the PEE membrane, which was attributed to its thinner active layer and higher affinity for water. Water flux could be increased by increasing the magnitude of the vapor pressure gradient across the membrane. This was a function of temperature and the relative

humidity of the air on the permeate, or posterior, side of the membrane. Water flux decreased as the TDS concentration of the feed solution approached 100 g L^{-1} . This was attributed to the formation of a concentration polarization boundary layer at the membrane surface. Nevertheless, water fluxes were maintained even at these high salt concentrations. The pervaporation membranes were capable of desalinating produced water samples from active well sites without any pretreatment for organic removal. Both the PEE and CTA membranes displayed excellent salt rejection capabilities (rejection $\geq 99\%$) independent of the salt concentration, or chemical makeup, of the feed solution.

The performance of the subsurface pervaporation irrigation system was evaluated using bench-scale grow box experiments and field trials. Alfalfa served as the vegetation in the grow box and field trial experiments. The tubular pervaporation membranes were found to show consistent water fluxes regardless of feed water salinity. The soil type and soil moisture influenced the water flux. Soils, like clays or clay loams, that are capable of wicking away moisture from the irrigation tubing are ideal for use of the pervaporation irrigation system. Fluxes were however found to generally increase as the relative humidity and surrounding soil moisture decreased. Alfalfa could be grown using the subsurface pervaporation irrigation system; however, supplemental surface watering will be required immediately following planting so that the plant root system may be established. Salt concentrations were found to increase during membrane operation, indicating good salt rejection capabilities and the potential for long-term use as a subsurface irrigation system.

Based on the results from this study we have determined that subsurface pervaporation irrigation is a feasible produced water management option for small producers. This conclusion is based on the demonstrated water flux and salt rejection capabilities of the two pervaporation membranes studied here. Of note, is that the CTA membrane displayed superior water flux characteristics to the PEE membrane. The suitability of this technology for a given application will be determined by the availability of land on which to install the irrigation system, amount of water requiring disposal, and the relevant climatic conditions. It is best suited for semi-arid and arid climates that are characterized by unsaturated soils. Such conditions will maximize the volumes of produced water that can be disposed of (concentrated down) using the irrigation system. Water flux will similarly be maximized through integration of water intensive vegetation, which will maintain

low soil moisture content, and thus a high vapor pressure gradient across the membrane. Further development and optimization of the membrane materials is needed to increase the characteristic water flux and durability of the irrigation membranes. These advancements will increase the diversity of produced water management applications for this technology.

INTRODUCTION

The development and evaluation of novel treatment technologies for managing oil and natural gas produced waters in environmentally sound and sustainable manners is needed to improve the ability of small energy producers to continue the development of our nation's energy resources. Therefore, the goal of this project is to provide small producers with a critical engineering assessment of a pervaporation based irrigation technology for treating produced water in geographically diverse locations. To meet this goal the following objectives were established for this project, and include:

OBJECTIVES

The goal of this project was to provide small producers with a critical engineering assessment of a pervaporation based irrigation technology for treating produced water in geographically diverse locations. To meet this goal the following objectives were established for this project, and included:

1. Assess critical process design and operation issues associated with using the pervaporation irrigation process for treating oil and natural gas produced waters.
2. Develop engineering and design information for implementing the pervaporation irrigation process in demonstration scale test systems.
3. Provide performance data for the pervaporation irrigation system in treating oil and natural gas produced water.
4. Create a user-friendly model for assessing the feasibility of implementing the pervaporation treatment process at geographically diverse field sites.

BACKGROUND

OIL AND NATURAL GAS PRODUCED WATERS

Produced water, sometimes referred to as formation water, is water that is co-produced during oil or natural gas exploration and extraction activities. It includes water derived from the reservoir in the formation, and water that is injected into the formation to facilitate oil and gas production [1, 2]. In 2007 between 15 to 21 billion barrels of produced water were generated in the United States. Of this amount, onshore oil and natural gas production accounted for the majority (95%) of domestic produced water generation [2, 3, 4]. As the pace of domestic energy development accelerates the volumes of produced water that must be managed will only increase. It is therefore imperative that management strategies be developed that are efficient at removing salts/minerals and cost effective, particularly for small energy producers.

The two most common methods of onshore produced water treatment are deep-well injection and evaporation ponds. Deep well injection is used for managing roughly 98% (volume basis) of the produced water that is generated domestically. Produced water is injected to maintain the formation pressure in oil/gas producing formations, or sometimes into non-producing formations for disposal. Evaporation ponds are the second most commonly used approach, albeit the less favored option, for disposal of produced water. Here water is placed in open pits and allowed to evaporate leaving behind precipitated solids. The size and cost of this option is a function of numerous environmental variables (evaporation rate, wind speed, temperature) and the amount of water to be disposed of. While effective, these options do not allow for the beneficial reuse of the produced water and are not always feasible for small producers. Further complicating the issue is the motivation to beneficially reuse produced waters, particularly in arid regions of the United States.

Competition for water resources by various stakeholders is intensifying, particularly in water poor areas where a lot of domestic resource extraction is occurring, putting pressure on the energy industry to maximize the beneficial use of produced waters when possible [2]. Meeting

this need requires that new treatment approaches and technologies be developed that meet the unique needs of the produced water market.

TREATMENT METHODS FOR PRODUCED WATERS

Methods for managing produced waters include passive treatment options (evaporation ponds), ion exchange, pressured driven membrane processes (nanofiltration and reverse osmosis) and non-pressure driven membrane processes (forward osmosis and membrane distillation) [5-9]. Mechanical evaporation and brine crystallization are also options for high salinity produced waters; however, costs and process complexity prevent these technologies from generally being options for small producers. A summary of the operating mechanisms, advantages and drawbacks of the various disposal and treatment technologies that are commonly used for managing produced waters is given in **Table 1**. In general, membrane processes have been limited in their application by membrane fouling, high energy requirements (kWh/gal), low water recoveries for highly saline source waters, and/or complexities that prevent their deployment in small-scale applications.

Table 1 - Summary of select disposal methods and treatment technologies typically used for managing produced waters.

| Technology | Operating Mechanism | Advantages | Drawbacks |
|-------------------------------|---|---|--|
| Evaporation Ponds [5, 10, 11] | Placing produced water in a pond, pit or lagoon with a large surface area to allow transformation of water in liquid form to vapor in the air. Dissolved and suspended solids remain in the pond following evaporation and require some form of disposal or capture for reuse | Simple design with minimal pretreatment and labor requirements | Land requirements may be substantial; Can lead to accumulation of increased concentrations of trace metals; Leaks in detention pond could cause groundwater pollution. |
| Ion Exchange [12-14] | Ions are exchanged between an ion containing solution and a bed of synthetic resin beads pre-saturated with non-contaminant ions. | Treatment results in high quality water for reuse; High water recovery (>90%) which means low brine volume requiring disposal | Substantial pretreatment may be required (i.e., removal of suspended solids, organics and hydrocarbon products) to prevent resin fouling; System design can be complex; resin beads must |

| | | | |
|--|---|---|---|
| | | | be regenerated |
| Nanofiltration / Reverse Osmosis [13, 15-17] | <p>A semi-permeable membrane is used to separate water from dissolved constituents based on differences in solubility and diffusion.</p> <p>NF (i.e., membrane softening) processes have high rejection efficiencies for multivalent ions and lower efficiencies for monovalent ones.</p> <p>RO has high rejection efficiencies for both mono- and multi-valent ions.</p> | <p>Removes both multi-valent and monovalent ions from water.</p> <p>Technology is modular; NF processes may be used upstream of RO to remove scale forming elements thus increasing the achievable recovery for the RO process.</p> | <p>Pressure requirements limited by the osmotic pressure of the feed water which means high salinity waters lead to lower recovery rates for the system; Membrane fouling can require extensive pretreatment systems; Complex operations could be challenging for small producers</p> |
| Forward Osmosis [18-22] | <p>Utilizes an osmotic agent on the draw side of the membrane to encourage the water to move across a semi-permeable membrane from low osmotic pressure to a high osmotic pressure side. The osmotic agent is then removed from the draw solution to leave behind the treated water.</p> | <p>Hydraulic pressure requirements (10-30 psi) are considerably less than pressure-driven membrane processes; Less susceptible to membrane fouling relative to pressure-driven applications.</p> | <p>Few full-scale treatment; Membrane materials are still in the infancy stage; Performance (flux) based on solubility/osmotic pressure of osmotic agent which may need to be removed/recovered from permeate stream after filtration takes place</p> |
| Membrane Distillation [19, 23-26] | <p>Distillation process in which the liquid-vapor interface is created by a hydrophobic, micro-porous membrane. Volatiles (water, etc.) evaporate across the membrane and are captured on the permeate side using a variety of configurations.</p> | <p>Not limited by the osmotic pressure of the feed solution and requires little pressure input. Little or no pretreatment required</p> | <p>Energy required to heat the water and cool/condense is high; No commercial membranes available or large scale applications exist (only pilot scale).</p> |

Beneficial Reuse

Population growth, and competition from different industrial interests, is placing unprecedented strain on limited freshwater supplies [1]. This pressure is a major driver for the development and implementation of beneficial reuse strategies for wastewater of various origins. The agricultural industry consumes a substantial fraction of domestic freshwater supplies. For example, crop irrigation accounts for roughly 39% of the total amount of fresh water consumption in the U.S. The large quantity of produced water generated from oil and gas production worldwide can be potential freshwater sources for various applications [4, 27]. One reuse option that has received considerable interest from produced water stakeholders, particularly in areas like Wyoming,

Colorado, and Texas, is irrigation of non-food crops. Reuse of produced waters in this way has the dual benefit of satisfying the industry's need to dispose of water, while satisfying the water needs of the agricultural industry. This in turn reduces the stresses that exist on the nation's water supplies.

Produced water can be a valuable resource for crop irrigation if we can lower its salinity, sodicity and toxicity to crops [27]. Produced water has been used for irrigation of crops in Wyoming and California. Coal bed methane (CBM) produced water was used in Wyoming by blending it with irrigation water and in some cases CBM water was used directly. Gypsum and other soil supplements have been used to maintain acceptable sodium absorption ratios in soils that have been irrigated with CBM produced waters. To facilitate the broader reuse of produced waters, including saline conventional produced waters, treatment systems that are simple in design and cost effective must be developed and implemented. This is particularly relevant to small producers for which large and costly treatment systems are not practical. Pervaporation irrigation is one such technology that combines treatment with the reuse application (i.e., irrigation of non-food crops)

PERVAPORATION

Pervaporation is a separation process which involves the separation of mixtures based on differing rates of diffusion and solubility in a non-porous membrane, followed by an evaporative phase change. Transport across the membrane occurs in three steps – attachment of solvent to the membrane surface, followed by diffusion of solvent across the membrane and a final step in which the permeate (vapor) desorbs from the posterior side of the membrane [28, 29]. It is a contraction of the terms permeation and evaporation because the feed is a liquid, and vapor exits the membrane on the permeate side as shown in **Figure 1**. Separation mechanisms are similar for pervaporation systems as those used in NF and RO. Separation of dissolved substances from water occurs because of differences in solubility in the polymer matrix and rates of diffusion.

Mass transport is achieved in pervaporation by lowering the activity of the permeating component on the permeate side through: gas carrier, vacuum or temperature difference. The driving force for pervaporation is the partial pressure difference of the permeating component

between the feed and permeate streams. The vapor pressure on the posterior side of the membrane (permeate side) must be lower than that on the feed side of the membrane for water to be transported across the membrane. This difference in vapor pressure is referred to as a vapor pressure gradient. Because the process utilizes differences in vapor pressure, rather than hydraulic pressure, it is classified as a non-pressure driven membrane process. As such, it may be used to desalinate source waters that are not suitable for treatment by NF and RO, which must overcome the osmotic pressure of the feed solution. Therefore, pervaporation may be a suitable alternative for treating highly saline produced waters where the TDS concentration may be $> 50,000$ mg/L. Pervaporation is also an attractive option for produced waters because as a non-pressure driven process it is expected to be more resistant to organic fouling.

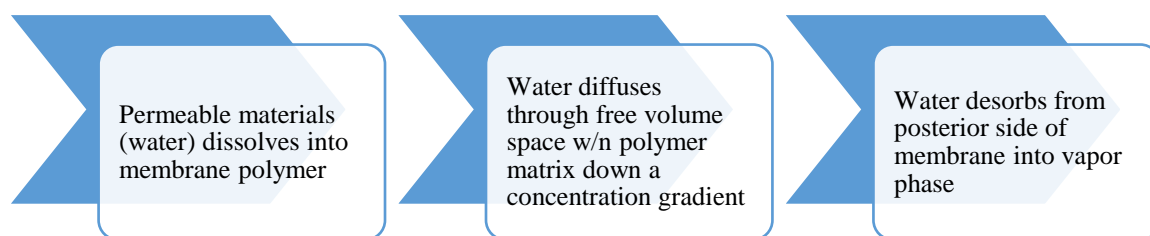


Figure 1 – Conceptual illustration of the pervaporation process involving a hydrophilic membrane

PERVAPORATION IRRIGATION SYSTEM

Pervaporation has been in use since the 1950s, though it has been traditionally used for alcohol dehydration [31-38] and removing volatile organics from water [39-41]. These historical applications of pervaporation have generally employed hydrophobic membranes to facilitate organic transport across the membrane while retaining the water in the feed stream. Interest in using pervaporation for desalination applications has recently increased [42-52]. For desalination applications pervaporation membranes must readily transport water, while readily rejecting dissolved salts and minerals. Desalination applications must therefore use hydrophilic

membranes. Use of pervaporation in subsurface irrigation applications is a new take on membrane processes because instead of being housed in a module or element the membrane is deployed in the ground.

Previous investigations [46-48, 51, 53, 54] have examined subsurface pervaporation using impaired source waters as a feed. These studies have collectively found that it is possible to supply the water requirement for typical crops such as tomato, pepper, and cucumber using impaired and/or saline source waters. These previous efforts [46-48, 51] have determined that a vapor pressure gradient is maintained across the pervaporation membrane through a variety of avenues. In the vapor/condensate from the tubular membrane is taken up by plant root systems. The second mechanism involves the transpiration of water vapor/condensate from the soil due to evaporation. Both mechanisms work to maintain a relatively constant moisture content, and in turn vapor pressure value, in the soil surrounding the irrigation tube.

Quinones et al. [46, 47, 51] determined that water flux increased with decreasing humidity in the vapor or gas phase, achieving a max flux of $3.99 \times 10^{-3} \text{ m}^3 \text{ m}^{-2} \text{ day}^{-1}$. Water flux was found to decrease with increasing feed water salinity. This was attributed to concentration polarization at the membrane surface and possible interference with water dissolution into the membrane polymer. Quinones et al. [47, 51] examined the performance of a pervaporation membrane in a soil box configuration, where the membrane was buried in two types of soil (a loamy soil and a loamy sand). A desiccant was used to simulate the plant root system and to maintain a relatively constant humidity value on the posterior side of the membrane. Water flux was found to be dependent on the soil moisture content, with the flux decreasing with an increase in soil moisture. These previous efforts have demonstrated that subsurface pervaporation irrigation is a viable technology for treating saline source waters while providing water for different crops. What remains to be determined is the suitability of this technology when using produced waters as a feed source.

EXPERIMENTAL METHODS

MEMBRANES

As part of this project we studied two different types of pervaporation membranes: a hydrophilic polyetherester membrane (PEE) and a hydrophilic cellulose triacetate membrane (CTA). Membranes were characterized in terms of their surface chemistry properties (by contact angle analysis and swelling analysis) and surface morphology (field electron scanning microscopy). The PEE membrane is a proprietary polymeric non-porous membrane that has been investigated by a variety of researchers for irrigation purposes (see [55],[51],[47, 56]). The PEE membrane was available in both flat-sheet and tubular configurations. The flat-sheet samples came in a variety of thicknesses (**Table 2**). The flat-sheet samples were used to characterize the basic performance properties (water flux and ion rejection) under controlled conditions using a flat-sheet test cell and a sweeping gas setup (Bench-scale pervaporation tests). The tubular membrane samples were corrugated tubes with a diameter of approximately 2.14 cm; tube samples of different linear density (i.e., number of corrugations per meter length of tubing) were examined (see **Table 2**). The tubular PEE membranes were used in the soil box experiments as described later. Field emission scanning electron microscopy images (FESEM) and energy dispersive x-ray analysis (EDS) of the virgin pervaporation flat-sheet and tubular membranes is described later in this report (see **Figure 6**).

A hydrophilic cellulose triacetate (CTA) membrane was also studied to develop a comparative performance analysis to the PEE membranes. The CTA membrane is a composite membrane with an active layer thickness of approximately 10 μm , and total thickness of about 115 μm . The density of the CTA membrane was approximately 1.31 g cm^{-3} (**Table 2**). Field emission scanning electron microscopy (FESEM) images and energy dispersive x-ray analysis (EDS) of the virgin CTA membranes can be seen (**Figure 7**).

Table 2 - Summary of select physical properties for the flat-sheet (second installment) and tubular forms of PEE and CTA membranes.

| | | | | |
|----------------------|-------------------|--|-------------------------------|---|
| PEE Membranes | Flat-Sheet | Thickness, μm | | Density, g cm^{-3} |
| | | 20, 50, 90, 250 | | 1.19 |
| | Tubular | Top Corrugation, mm | Bottom Corrugation, mm | Linear Density, g m^{-1} |
| | | 0.4 | 0.9 | 90 |
| | | 0.3 | 0.7 | 70 |
| | | 0.2 | 0.6 | 56 |
| CTA Membranes | Flat-Sheet | Thickness, μm | | Density g cm^{-3} |
| | | Active Layer | Total Thickness | 1.31 |
| | | 10 | 115 | |

Membrane Surface Chemistry - Contact Angle Measurements

Contact angle measurements were performed using an Easy Drop Goniometer (Krüss Scientific) on the flat-sheet membrane samples to characterize their relative hydrophobicity. Surface energy values for the different membranes studied here, to include the van der Waals (γ^{LW}) and Lewis Acid-Base (γ^+ , γ^-) components, can be calculated using contact angle data and the approach outlined in Brant and Childress [57].

The captive bubble technique was used to measure the contact angles for water on the different membrane samples. The left, right and average contact angle values were measured for each liquid droplet. A minimum of five liquid droplets were analyzed on three different membrane samples resulting in a minimum sample population of 15 contact angle results per probe liquid and membrane. Values were discarded if the measured left and right angles disagreed (\pm) by more than 2° . A large difference between the left and right contact angle could indicate that the membrane surface was not perfectly flat and/or that the liquid droplet was interacting with an imperfection (or contamination) on the membrane surface. Captive bubble measurements were completed for the contact angle measurements with water because this approach allowed the membrane to stay in a hydrated condition. The sessile drop technique was used to measure the contact angles for the formamide and diiodomethane on the PEE and CTA membranes.

Water Uptake by Pervaporation Membranes - *Swelling Analysis*

A swelling analysis was performed on the tubular and flat-sheet PEE membrane samples to determine the amount of water that is absorbed by the material. For the swelling analysis samples of the PEE membrane tubing were cut into approximate lengths of 2.5 cm. Each membrane sample was weighed (dry) using a mass balance and its length and diameter measured using digital calipers. The tube samples were then submerged in aqueous solutions of varying ionic strength using unbuffered doubly deionized water (DDW) and reagent grade NaCl. The DDW was characterized by an average pH = 5.5 and a resistivity = 18 m Ω -cm. Three PEE membrane tube samples ($n = 3$) were analyzed in each of the following test solutions: DDW, 0.001 M NaCl, 0.010 M NaCl, 0.10 M NaCl, and in the Dutch Creek CBM produced water (pH = 8). Note that the CBM produced water was the same as that used in the soil box and field tests. The pH of the DDW and the three different NaCl solutions was approximately 5.5; all tests were conducted at room temperature ($T = 24^{\circ}\text{C} \pm 2^{\circ}\text{C}$). A similar swelling analysis was performed using the flat-sheet PEE membranes. Three samples of each membrane thickness (20, 50, 90 and 250 μm) were weighed (dry) and then submerged in solutions of varying ionic strength. The following test solutions were used: DDW, 0.01M NaCl, 0.10 M NaCl, 1.0 M NaCl and the Dutch Creek CBM water (pH = 8). The flat-sheet samples were periodically removed from the test solution over a total of three days to be weighed. The excess water on the membrane surface was removed by lightly dabbing each side of the membrane with a kimwipe. The pH of the DDW and the three different NaCl solutions was approximately 5.5; all tests were conducted at room temperature ($T = 24^{\circ}\text{C} \pm 2^{\circ}\text{C}$).

Pervaporation Membrane Surface Morphology - *Scanning Electron Microscopy (SEM)*

A table top scanning electron microscope (SEM) (Hitachi TM-1000, Hitachi High Technologies America, Inc., Pleasanton, CA) was used to take images of dry and wet flat-sheet pervaporation samples as to characterize any changes in surface morphology that might occur as the polymer swelled. The samples were cut using scissors and attached to the sample stage using double sided carbon tape. The wet sample was soaked in DDW (pH approximately 5.5) for ≥ 24 hrs prior to being imaged. Three areas were randomly selected for imaging on each surface to make sure that the membrane surface was uniform.

Field emission scanning electron microscope (FESEM) images (Quanta FEG MK2 Scanning Electron Microscope, FEI, Eindhoven, The Netherlands) were taken along with energy dispersive X-ray analysis (EDS) (Oxford Instruments X-Max EDS Detector, Model #51-XXM0005, Concord, MA, USA) to characterize the elemental composition of the virgin PEE and CTA membrane materials. Representative images were also taken and elemental analysis was performed on the surface and cross section of each membrane after performing experiments to determine if contaminants were passing through the membranes during operation. When performing EDS analysis on the cross section of each membrane sample, elemental mapping was completed for both the entire surface of the cross section shown in the image as well as different lines throughout the thickness of the membrane sample to look for “salt fronts” within the membrane depth. Images of each sample were taken using two different methods: Everhart-Thronley detector (ETD) and back-scattered electron detector (BSED). ETD images show the shapes and textures of items that are in the image. BSED images show locations in the images that have higher average atomic number (Z) than the average Z of the sample. Locations in the image with proportionally high Z , for example a salt crystal on the surface of the membrane, appear brighter than the locations with lower Z values.

BENCH-SCALE PERVAPORATION EXPERIMENTS

Bench scale pervaporation tests were performed using the flat-sheet PEE and CTA membranes as a means of evaluating how membrane/environmental conditions relate to the performance of the membranes (flux, salt rejection capabilities). A schematic of the diffusion bench-scale experiments is given in **Figure 2**. The bench-scale pervaporation experiments can be described in terms of a liquid flow line and the air flow line. The liquid flow line (represented by blue lines in **Figure 2**) was a closed loop recycled liquid line where the concentrate from the diffusion cells was returned to the feed reservoir. The feed solution was placed in the jacketed-reactor feed reservoir, where it was mixed and the temperature was adjusted using a heat exchanger. After flowing through a flow meter, the liquid train was split into two lines, each with its own pressure gauge, before flowing into the pervaporation cells. Two pervaporation cells were used to increase the membrane surface area used during the experiments. Pervaporation membrane

samples were cut out with an X-Acto knife to fit the appropriate dimensions of the cell (**Figure 2**). The pervaporation membranes were placed into the cells dry so that a water tight seal between the membrane and pervaporation cell could be formed. After the pervaporation cells, the two lines were again merged into one liquid flow line before being returned to the feed reservoir. An inline conductivity probe was located just prior to returning the concentrate to the feed reservoir as a means of monitoring the feed/concentrate conductivity during the experiments. The airline flow of the bench-scale pervaporation experiments (represented by the red and green lines in **Figure 2**) was set up as a sweeping air configuration to maintain the vapor pressure on the permeate side of the membranes as low as possible and to collect the vapor permeate. The source compressed air was sent through a drierite column to remove any moisture in the air (air was assumed to have a relative humidity of 0% after going through the drierite column). The air flowed through an air flow meter (varying air flow velocities were used in these experiments) before being split into two separate lines to flow into the two different pervaporation cells. Inside the pervaporation cells, the permeate was collected by the feed airline and the combination of the two flows continued on to the liquid trap (red line in **Figure 2**). Liquid nitrogen was used to condense the permeate, which is in water vapor form within a condensing vessel, while the dried air was allowed to escape to the atmosphere (green line after liquid trap in **Figure 2**).

Once the experiment was completed, the condensing vessel was sealed and allowed to reach room temperature. The volume of water processed by the membrane was determined by weighing the condensing vessel before and after each test. The duration of each test was recorded. The permeate flux was determined by using values for the volume of water processed, surface area of the two membranes and duration of test as described in **Equation 1**. The flux of a substance, water or dissolved substance, through a membrane is given as:

$$J_i = \frac{V_i}{SA_m * t} \quad (1)$$

where J_i is the permeate flux of component i ($\text{m}^3 \text{m}^{-2} \text{day}^{-1}$); V_i is the volume of component I processed by the membrane (m^3); SA_m is the surface area of the feed side of the membrane through which component i is processed (m^2); and t is the time over which the permeation event took place (day).

The specific permeate flux of a substance is defined as the permeate flux normalized over the transmembrane pressure and is given as:

$$J_{isp} = \frac{V_i}{SA_m * t * P} \quad (2)$$

where J_{isp} is the specific flux, or permeability ($\text{m}^3 \text{ m}^{-2} \text{ day}^{-1} \text{ Pa}^{-1}$); P is the transmembrane pressure (Pa). When calculating the membrane permeability (specific flux of pure liquid water through membrane), the P value used in **Equation 2** is the transmembrane pressure (hydraulic pressure), or the difference in pressure present on the feed and permeate sides of the membrane. The transmembrane pressure was used to determine the membrane permeability in this research. However, as explained before the driving force for traditional pervaporation membrane experiments is the vapor pressure gradient ($p_{io} - p_{il}$). So, when the specific flux of the pervaporation membranes are determined during traditional pervaporation experiments (i.e., the permeate is in vapor form, not liquid) the vapor pressure gradient value would be used to determine the specific flux of the membrane.

The recovery (R) of a membrane system is the ratio of the amount of water that is produced by the system (treated) to the amount of water fed into the system (untreated water). This value is used to determine the efficiency, in terms of water treated, for the membrane system. Recovery is found by:

$$R = \frac{V_p}{V_f} \quad (3)$$

where R is the recovery of the system (unitless); V_p is the volume of the permeate produced by the system (m^3); and V_f is the feed volume of the membrane system (m^3). The rejection (r) capabilities of a membrane can be calculated for bulk parameters, like TDS or conductivity, or for specific salts/contaminants. Bulk conductivity measurements were primarily used in this research to measure rejection:

$$r = 100 * \frac{(c_f - c_p)}{c_f} \quad (4)$$

where r is rejection (%), c_f is the concentration of the feed solution (mS cm^{-1} or mg L^{-1}); and c_p is the concentration of the permeate (mS cm^{-1} or mg L^{-1}).

The concentration factor (CF) of a membrane process provides an indication of the degree to which the concentration of the concentrate/retentate (water that is not processed by the membrane) increases compared to the permeate (water that is processed by the membrane). This value is useful to know for membrane processes like RO which produce brine (concentrate) solutions which must be disposed of. The concentration factor can be found by:

$$CF = \frac{1}{1-R} \quad (5)$$

When evaluating pervaporation membranes, a value known as the enrichment factor (β_i) is often used to evaluate membrane rejection/selectivity characteristics. Mathematically, β_i can be expressed as:

$$\beta_i = \frac{c_{pi}}{c_{fi}} \quad (6)$$

where β_i is the enrichment factor (unitless); c_{pi} is the concentration of component i in the permeate (mS cm⁻¹ or mg L⁻¹) and c_{fi} is the concentration of component i in the feed (mS cm⁻¹ or mg L⁻¹).

Membrane samples were stored after completing the experiments for further analysis (FESEM-EDS). The categories of tests performed on this experimental setup include temperature profile experiments and rejection tests. Parameters that were varied during the bench-scale pervaporation experiments include feed water temperature (20, 25, 30, 40 and 50°C), feed water salinity/type (0, 10, 50 and 100 g L⁻¹ NaCl solutions as well as the Dutch Creek CBM, two produced waters, PW-I and PW-II) membrane thickness (20, 50, 90 and 250 µm) and membrane type (PEE and CTA flat-sheet membranes). The feed water temperature, membrane thickness, feed water salinity and membrane type were all varied in order to understand how each parameter affected the water flux through the pervaporation and CTA membranes.

The temperature profile experiments were conducted to determine the role that feed water temperature (i.e., vapor pressure difference) and membrane thickness play in the permeate fluxes through the PEE and CTA membranes. The feed water temperature used in each test was DDW (pH = 5.5). Tests were performed using the CTA membranes and PEE flat-sheet samples of different thicknesses ($l = 20, 50, 90$ and 250 µm) at different feed water temperature settings ($T =$

20, 25, 30, 40 and 50°C). Three samples of each membrane thickness were processed at each temperature. Water was filtered through the membranes for 2- hrs, during which time the vapor permeate was collected in the condensing vessel. The permeate was allowed to reach room temperature, and the mass of the collected permeate was measured in order to calculate the permeate flux value for each test.

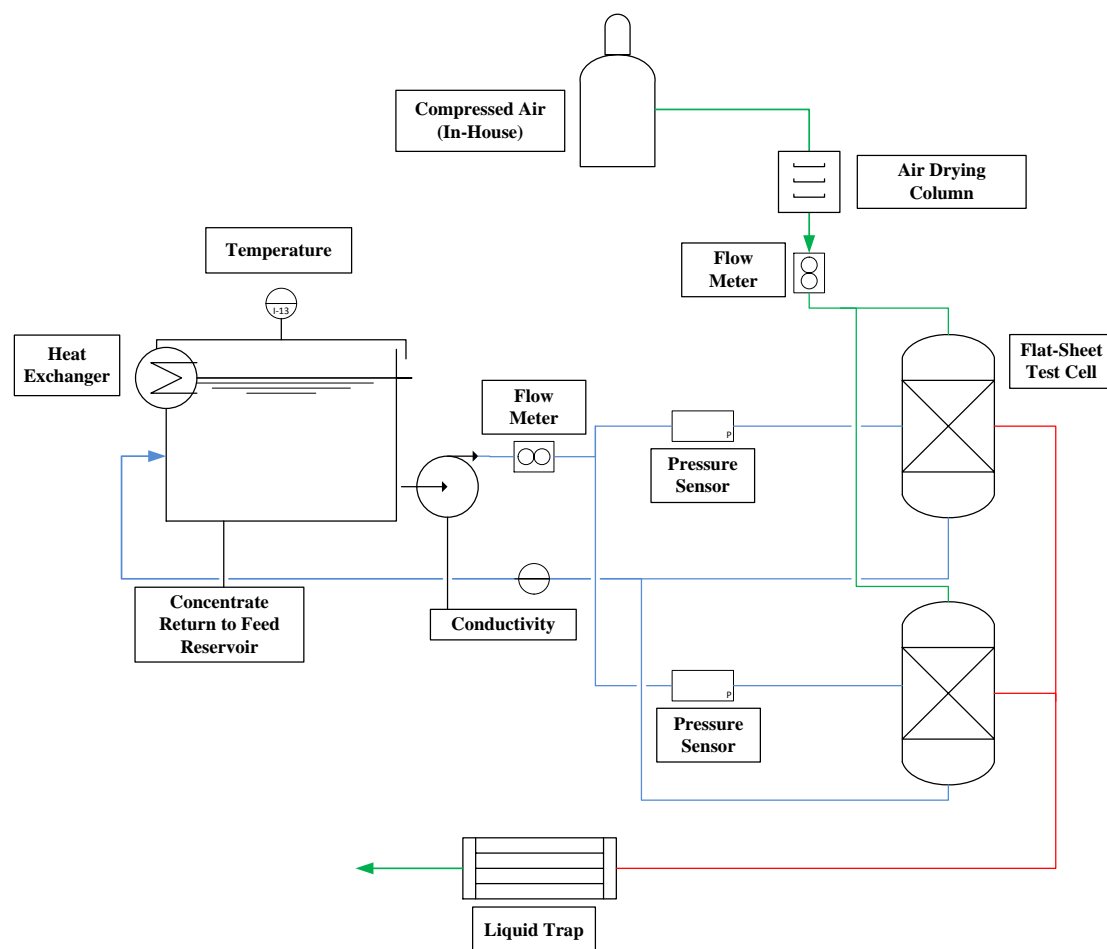


Figure 2 - Process flow diagram of the cross flow pervaporation test unit. Blue lines correspond to the liquid flow lines, green lines correspond to dry air flow lines and the red lines correspond to the air and water vapor flow lines.

Rejection experiments were performed to determine how well the pervaporation and CTA membranes separated solutes from water during operation. Feed solutions analyzed included: NaCl solutions at concentrations of 10, 50 and 100 g L⁻¹, a CBM produced water (see **Table 4**) and the two conventional produced water samples (see **Table 5**). During these experiments, the feed water temperature was maintained at 50°C. The collected permeate was allowed to reach room temperature, after which time the mass of the collected permeate was measured to calculate

the permeate flux value for each test. Conductivity and/or TOC measurements were performed on each permeate sample so that the membrane rejection could be calculated for each test (**Eq. 4**).

BENCH-SCALE SOIL BOX EXPERIMENTS

Bench-scale tests using the tubular form of the pervaporation membrane, referred to here as soil box experiments, were performed using a pervaporation irrigation process representative of a field installation, but under controlled environmental conditions. A schematic of the bench-scale system (i.e., the soil box) is given in **Figure 3**. The pervaporation tubing ($l = 1 \text{ m}$, $A = 1.103 \text{ m}^2$) was attached to the water tight fittings inside the box, at a depth of ten cm from the bottom, and surrounded by 0.25 m^3 of soil media (total soil depth was 20 cm from the bottom of the box). The total depth of the box was 30 cm, which means there was 10 cm of headspace (headspace volume = 0.13 m^3) within the box. Types of soil used in the experiments included washed silica sand, garden soil and a clay loam soil.

Feed water was placed in the feed reservoir from which it traveled into the pervaporation tubing. The feed tank was placed on a scale and the amount of water that was being processed by the tubing was determined from the change in mass of the feed tank. The feed tank was placed at an elevation above the tubing to provide some pressure head (approximately 2.8 kPa) to the pervaporation tubing. Conductivity, pH and temperature probes were placed in the feed tank to monitor these parameters throughout the experiments. Twelve soil probes were placed within the soil box at various depths and distances from the pervaporation tubing to monitor the soil moisture, soil conductivity and the soil temperature. Probes were also placed in the head space within the box to measure the temperature and relative humidity (RH) of the air above the soil. One probe was attached to the lid of the box and the other probe was placed on the soil surface to determine if a humidity gradient was present within the headspace. An airline was used to flow air through the box (flow rate = 1 L min^{-1}) as a means to keep the humidity in the soil box as low as possible. Samples were periodically drawn from inside the pervaporation tubing using a sample line that was fed into the pervaporation tubing. The conductivity of the drawn samples was measured as a way of monitoring the increase in salt concentrations in the reject line during

the experiments. In all nine different soil box tests were conducted at various conditions. The feed was recycled through the membrane using a peristaltic pump for tests 8 and 9.

The test conditions varied for each test included feed water type, soil type, pervaporation membrane thickness, test duration and temperature control (**Table 3**).

Table 3 - Summary of test conditions changed in each of the soil box bench scale experiments. Test conditions that were kept the same for each test include: airflow through soil box (1 L min^{-1}), depth of soil (20 cm), volume of soil (0.25 m^3), and depth of tubing within the soil (10 cm). PEE membranes of different thicknesses were used for tests 1-8. A CTA membrane was used for test 9. Additionally the feed water was recycled through the membrane tubing for tests 8 and 9.

| Test | Feed Water | Soil Type | Membrane Thickness, g m^{-1} | Duration, days | Water Temperature, $^{\circ}\text{C}$ |
|------|-----------------------|--------------------|---------------------------------------|----------------|---------------------------------------|
| 1 | Dutch Creek | Washed silica sand | 90 | 15 | 29.9 |
| 2 | Synthesized CBM water | Washed silica sand | 90 | 30 | 26.9 |
| 3 | Dutch Creek | Garden soil | 90 | 53 | 29.9 |
| 4 | Dutch Creek | Garden soil | 90 | 30 | 28.9 |
| 5 | Dutch Creek | Garden soil | 70 | 21 | 30.4 |
| 6 | Dutch Creek | Garden soil | 50 | 14 | 29.6 |
| 7 | Dutch Creek | Clay loam | 90 | 36 | 22.8 |
| 8 | Dutch Creek | Clay loam | 90 | 42 | 24.9 |
| 9 | Dutch Creek | Clay loam | - | 15 | 24.7 |

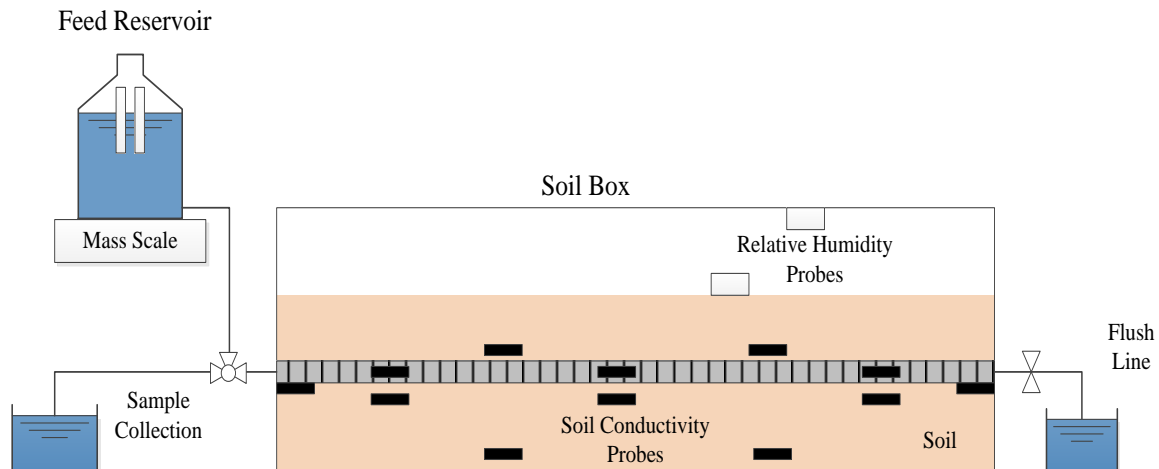


Figure 3 - Experimental set-up for the bench-scale pervaporation irrigation tests (soil box).

BENCH SCALE GROW BOX EXPERIMENTS

Bench-scale grow box tests were conducted using the tubular form of the cellulose triacetate membrane. The grow box tests represent a logical follow up to the soil box experiments to study the effect of the plants on the pervaporation process (crop water demand on the water flux across the membrane). They were also performed using a pervaporation irrigation process representative of a field installation, but under controlled environmental conditions. A schematic of the bench-scale system (grow box) is given in **Figure 4**. The soil used in this test was garden top soil. Alfalfa seedlings were transplanted into the soil. Grow supplements were regularly added to the soil when it was determined that the soil was deficient in potassium as indicated by the curling of the leaf tips and chlorosis (yellowing) between the leaf veins. Also, the plants were watered regularly as the single membrane in the grow box would not be able to provide sufficient water to all the plants. A 300 watt plasma grow light placed 2 feet above the soil surface served as the artificial light source. The spectrum provided by plasma grow lights is very close to that of sunlight. The light was operated using a timed power source and was operated on a 13 hour daylight basis. The feed water for the grow box tests was a synthetic produced water prepared using deionized water and NaCl and the TDS content was 2000 mg/L. The grow box differed from the soil box experiments in that the box was not sealed anymore (to grow plants). The amount of water processed by the membrane (mass loss in the feed tank), the various soil

characteristics (volumetric moisture content, electrical conductivity and temperature) and feed parameters (pH, conductivity and temperature) was continuously recorded using different probes similar to the soil box experiments. Samples were regularly drawn from inside the membrane to record the increase in conductivity which served as an indicator of the salt rejection within the membrane.

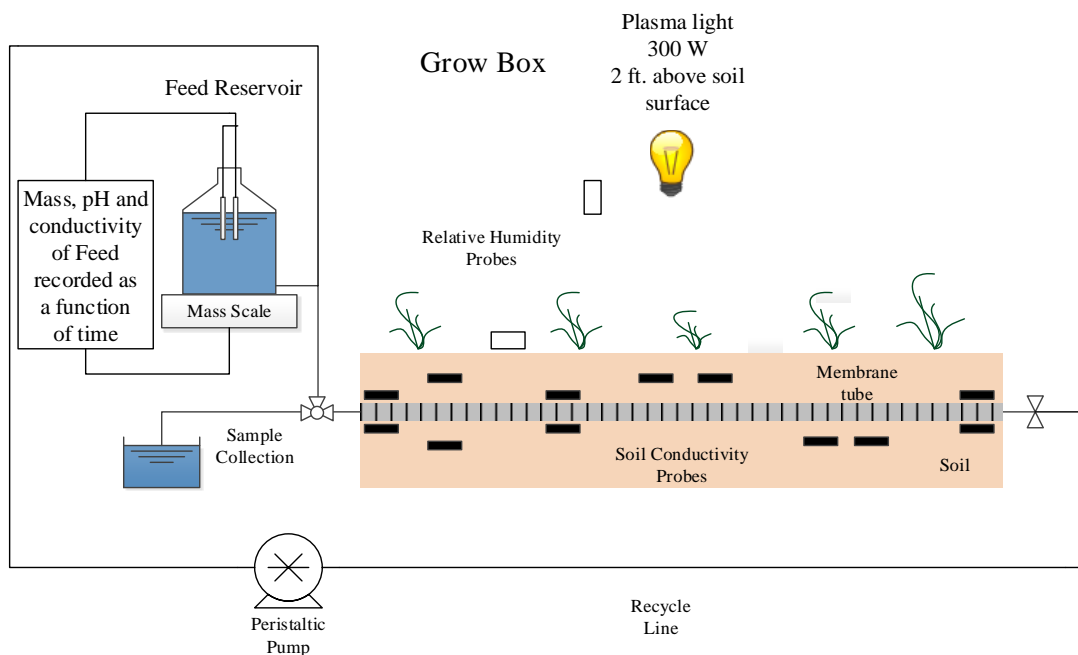


Figure 4 - Experimental set-up for the bench-scale pervaporation irrigation tests (grow box).

FIELD TRIALS

Field trials were conducted at the University of Wyoming's Agricultural Research Station in Sheridan, Wyoming. These tests were done using the tubular PEE membranes only. The study was designed to determine the effects of environmental conditions on the performance of the pervaporation irrigation system while growing alfalfa plants. Four test plots were used in the field trial: two control plots on which no plants were grown and two active plots on which alfalfa plants were grown. Alfalfa seedlings were grown at a greenhouse located at the research station. The seedlings were transplanted to the two active sites after approximately 10 days. Dimensions and the general layout of the test plots are given in **Figure 5**. The source water for the field trials

was CBM produced water that was collected from nearby CBM gas wells at the Dutch Creek site in Sheridan, WY. The tubular PEE pervaporation membranes were roughly 0.3 m below the grade. The feed water temperature, water elevation in the feed tank, and soil parameters (volumetric soil moisture, electrical conductivity and temperature) were all monitored continuously using a LabView designed data acquisition system. The locations of the soil conductivity probes were spatially varied in order to develop a moisture profile from the tubular membranes. The soil in which the tubular membranes were buried was characterized as silty clay loam. A weather station at the field site was used to measure and record the following weather parameters: wind speed, sunshine, rainfall, temperature, and relative humidity.

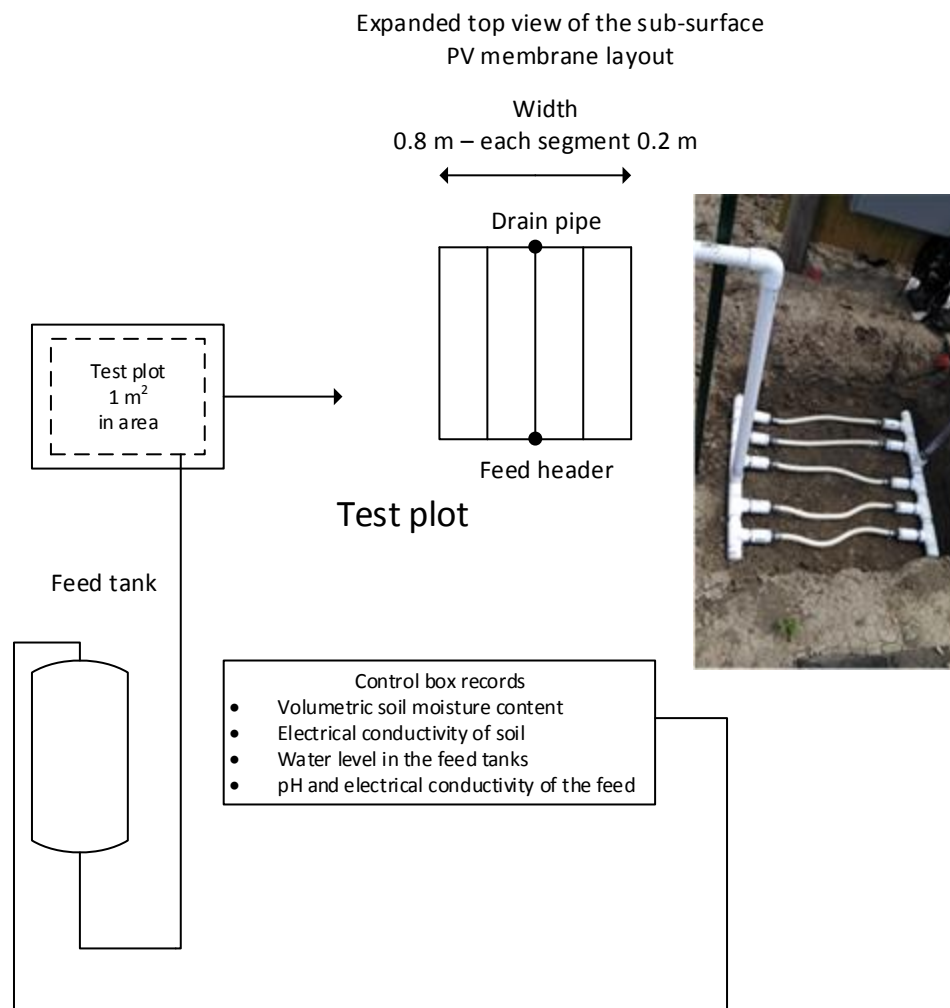


Figure 5 – Diagram and layout of the test plots used in the field trials of the pervaporation irrigation system.

COALBED METHANE (CBM) AND CONVENTIONAL PRODUCED SOURCE WATERS

Samples of CBM produced (**Table 4**) and conventional produced (**Table 5**) waters were collected from various active well sites and subsequently used in a variety of pervaporation experiments. The CBM water samples were collected from an active CBM produced water detention pond in the Powder River Basin, WY from a location called the Dutch Creek Site near Sheridan, WY. Produced water samples were collected from the Dutch Creek field site and sent to Wyoming Analytical Laboratory (WAL) for an analysis including the following measurements: pH, TDS, TOC, ions of interest (Na^+ , Ca^{2+} , Mg^{2+} , Cl^- , SO_4^{2-}) and metals of interest (B, Fe, Zn, and Li). Historical water quality values (measured in December of 2010) for the CBM water are also included in **Table 4**. These values were included to determine if the water quality of the Dutch Creek CBM produced water was remaining relatively constant over time. The detention pond is currently being used to store untreated produced water from multiple active CBM wells in the Sheridan, WY area prior to it being treated (by acidification) and subsequently used for subsurface irrigation of alfalfa. Water samples were collected from the feed pipes to the detention pond periodically throughout the research project (approximately every 4 months). The collected water samples were stored in Nalgene containers and stored in a cold dark room ($T = 5^\circ\text{C}$) to prevent biological growth. Samples of the CBM produced water were used in pervaporation experiments without any purification or pretreatment. The CBM produced water was clear and lacked any color, indicating a relative lack of natural organic matter (NOM). The average pH of the CBM water was 7.9 ± 0.2 , which is consistent with other CBM water from basins across Wyoming. The mean TDS concentration in the CBM produced water was approximately $1,500 \text{ mg L}^{-1}$, and as such is characterized as a brackish water. The TDS is primarily composed of sodium (Na^+) and bicarbonate (HCO_3^-) ions. As the CBM water becomes more concentrated, the HCO_3^- concentration increases which results in a pH increase. A reduction in the Na^+ concentration would facilitate the beneficial reuse of the CBM water because it would decrease the SAR of the water making it less of a hazard to the soil structure and vegetation health; a reduction in HCO_3^- concentration would keep the pH in a neutral zone and aid in removing carbonates from the system, which are likely scale forming compounds. The total hardness of the water was calculated to be 66.2 mg L^{-1} as CaCO_3 , which classifies the CBM

water as a soft water according to the U.S. EPA's classification system for water hardness [59]. The TOC concentration in the CBM water was 19 mg L^{-1} , which is very high compared to other CBM waters in Wyoming.

Table 4 - Select water quality measures for the CBM produced water from the Dutch Creek site in Sheridan, WY.

| Water Quality Parameter | Units | Measured Value | Historical Value |
|-------------------------------|----------------------|-----------------|------------------|
| pH | - | 7.91 ± 0.28 | 8.1 |
| Color | - | None (Clear) | - |
| Conductivity | mS cm^{-1} | 2.120 | 2.08 |
| Total dissolved solids (TDS) | mg L^{-1} | 1230 | 1290 |
| Total organic carbon (TOC) | mg C L^{-1} | 19 | |
| Cations and Anions | | | |
| Na ⁺ | mg L^{-1} | 444 | 539 |
| Ca ²⁺ | mg L^{-1} | 10 | 6 |
| Mg ²⁺ | mg L^{-1} | 10 | 3 |
| Cl ⁻ | mg L^{-1} | 6 | 6 |
| SO ₄ ²⁻ | mg L^{-1} | 36 | 7 |
| HCO ₃ ⁻ | mg L^{-1} | 1234 | 1440 |
| Metals | | | |
| B | mg L^{-1} | 0.229 | 0.1 |
| Fe | mg L^{-1} | 0.3 | 0.47 |
| Li | mg L^{-1} | 0.151 | 0.2 |
| Zn | mg L^{-1} | 0.002 | 0.01 |

Conventional produced water samples were collected from two oil producing wells in Texas. The samples are denoted as PW1 and PW2 to protect the confidentiality of the source wells. Both produced water samples were delivered in opaque drums and were stored until they were used in a cold room at $T = 5^{\circ}\text{C}$. The produced water samples were not treated (e.g., filtered) prior to use in the pervaporation experiments. Water quality for the produced water samples from the two oil wells are summarized in **Table 5**. Both water samples had a cloudy appearance and had noticeable odors. The PW1 and PW2 samples had TDS concentrations of 77,385 and 60,049 mg

L⁻¹, respectively, with the primary constituents being sodium and chloride. The total hardness of the PW1 and PW2 samples were 11,878 and 1,167 mg L⁻¹ as CaCO₃, respectively. Therefore, both produced waters are characterized as very hard waters, with the PW1 being extremely hard. The TOC concentrations in the PW1 and PW2 samples were 180 and 1,240 mg L⁻¹, respectively. Oil and grease, was found to be 42 mg L⁻¹ in the PW2 sample, and nearly none (<0.1 mg L⁻¹) in the PW1 sample.

Table 5 - Select water quality values for the two conventional produced water samples. All water quality measurements were done by the Wyoming Analytical Laboratory (WAL), with the exception of pH, conductivity and total dissolved solids analyses.

| Parameter | Unit | PW1 | PW2 |
|------------------------|---|--------|--------|
| pH | | 7.09 | 7.87 |
| Conductivity | mS cm ⁻¹ | 115.5 | 89.62 |
| Total dissolved solids | mg L ⁻¹ | 77,385 | 60,049 |
| Sodium | mg L ⁻¹ | 34,660 | 32,800 |
| Calcium | mg L ⁻¹ | 3,212 | 436 |
| Magnesium | mg L ⁻¹ | 934 | 128 |
| Iron | mg L ⁻¹ | 0.059 | 0.662 |
| Bicarbonate | mg L ⁻¹ as CaCO ₃ | 175 | 608 |
| Chloride | mg L ⁻¹ | 53,200 | 37,100 |
| Sulfate | mg L ⁻¹ | 2 | 2 |
| Total Organic Carbon | mg L ⁻¹ | 180 | 1,240 |
| Oil and Grease | mg L ⁻¹ | <1.0 | 42 |

RESULTS AND DISCUSSION

MEMBRANE SURFACE CHEMISTRY

Membrane Affinity for Water

The affinity of membrane materials for water is an important factor for predicting water flux in desalination applications. This was measured using contact angle analysis and water adsorption experiments. Membrane surface chemistry (hydrophilicity) dictates how membranes interact with water and other substances (salts, organics) that may be in feed solution. Contact angle and surface energy values for the CTA membrane and the flat-sheet PEE membranes samples are summarized in **Table 6**. Both membranes were hydrophilic based on the values of their contact angle with water ($\theta \ll 90^\circ$). Contact angles with water were measured on each of the various thicknesses of the PEE membranes (**Table 6**). This was done to evaluate if the membrane chemistry varied between, which could affect membrane performance. Statistical analysis (completely randomized design [CRD] one way analysis of variance [ANOVA]) was performed and it was determined that there was no significant difference between the average contact angle with water for the PEE membranes of different thicknesses. This allows for the assumption that any observed differences in PEE membrane performance were due to differences in membrane thickness. Both the CTA and PEE membranes were characterized by high electron donor components (γ^-) and comparatively lower electron acceptor components (γ^+) (**Table 6**). A high γ^- component means that there is a large amount of negatively charged sites on the membrane material for particles to attach to compared to a low amount of positively charged sites present on the membrane (due to a low γ^+). Both membranes were found to have positive interfacial free energy values with water (ΔG_{sws}), indicating that they are both strongly hydrophilic in agreement with the contact angle with water results.

Table 6 - Summary of contact angle values for the water, formamide, and diiodomethane probe liquids on the CTA and flat-sheet PEE membranes ($T = 24^{\circ}\text{C}$, $\text{pH} = 5.5$, $I = 0.0 \text{ M}$; $n = 15$).

| | Contact Angle | Surface Energy Components |
|----------------------------------|------------------|---|
| CTA Membrane | | |
| Water | 11.8 ± 4.70 | $\gamma^{\text{LW}} = 36.43 \text{ mJ m}^{-2}$ |
| Formamide | 19.44 ± 4.12 | $\gamma^{\text{AB}} = 17.45 \text{ mJ m}^{-2}$ |
| Diiodomethane | 46.1 ± 6.85 | $\gamma^{+} = 1.34 \text{ mJ m}^{-2}$ |
| | | $\gamma^{-} = 56.59 \text{ mJ m}^{-2}$ |
| | | $\Delta G_{\text{SWS}} = 34.75 \text{ mJ m}^{-2}$ |
| PEE Membrane | | |
| 20 μm + Water | 46.1 ± 2.97 | $\gamma^{\text{LW}} = 35.93 \text{ mJ m}^{-2}$ |
| 20 μm + Formamide | 59.3 ± 4.78 | $\gamma^{\text{AB}} = 11.46 \text{ mJ m}^{-2}$ |
| 20 μm + Diiodomethane | 47.0 ± 3.03 | $\gamma^{+} = 0.59 \text{ mJ m}^{-2}$ |
| 50 μm + Water | 46.2 ± 2.61 | $\gamma^{-} = 55.26 \text{ mJ m}^{-2}$ |
| 90 μm + Water | 48.2 ± 2.74 | $\Delta G_{\text{SWS}} = 37.29 \text{ mJ m}^{-2}$ |
| 250 μm + Water | 48.4 ± 5.12 | |

Water adsorption measurements were used to give insight on how constituents, specifically salts, might affect the interaction(s) between water molecules and the membrane polymer. Results from this analysis for the tubular PEE membranes are summarized in **Table 7**. Measurements were not done for the CTA membrane. The results shown are the change in membrane mass and dimension following soaking in DDW for 3 days. The mass of the tubular PEE membranes reached a maximum (or maximum amount of water absorption) after approximately 24 hrs. The PEE membranes thus readily adsorbed water irrespective of solution ionic strength; however, the change in membrane mass decreased with increasing solution ionic strength. This suggests that the salts (sodium and chloride) affected the interaction between the water molecules and the membrane polymer chains, although the exact mechanism(s) by which this affected the amount of water that could be adsorbed by the polymer remain unclear. In addition to an increase in mass the dimensions of the tubes also increased as they adsorbed water (Table 7). The increase in the length of the tubes remained constant across all conditions at approximately 10%.

Table 7 - Fractional increase in mass due to water uptake for the pervaporation tubing at the end of 3 days in solutions with varying ionic strength. The data shown are the final measurements taken of the samples (pH of DDW = 5.5, pH of CBM water = 7.9, T = 24°C, n = 3).

| Solution | Mass Increase of Pervaporation Tubing, % | Length Increase of Pervaporation Tubing, % | Diameter Increase of Pervaporation Tubing, % |
|------------------------|---|---|---|
| DDW | 48.47 ± 1.2 | 10.77 ± 0.9 | 9.67 |
| 1 mM NaCl | 40.45 ± 2.6 | 10.05 ± 0.3 | 11.11 |
| 10 mM NaCl | 36.95 ± 1.0 | 10.32 ± 1.2 | 10.39 |
| 100 mM NaCl | 35.50 ± 0.7 | 10.22 ± 1.3 | 9.96 |
| CBM Water (I ~ 0.022M) | 35.44 ± 2.5 | 10.66 ± 1.3 | 8.23 |

Physical Characteristics and Elemental Composition of the CTA and PEE Membranes

Field emission scanning electron microscopy (FESEM) images and energy dispersive x-ray analysis (EDS) were taken/performed for the virgin pervaporation (flat-sheet and tubular) and CTA membranes in order to determine the morphology and composition of the different membranes. Images and EDS analysis of the film blown flat-sheet PEE membranes can be seen in **Figure 6**. Surface and cross section images of the 20 and 250 µm thick PEE membranes are shown (**Figure 6[a]-[d]**). The PEE membranes were observed to be homogeneous/symmetric membranes, meaning that the structure and composition of the membrane is the same throughout its entire thickness. A representative EDS analysis (**Figure 6[e]**) of the PEE membranes shows that they were primarily composed of carbon and oxygen, with trace amounts of sodium, calcium, potassium, chlorine and titanium. Virgin tubular PEE membranes were also analyzed using FESEM-EDS (not shown here). There were no noticeable layers in the membrane cross section or irregularities on the tubular membrane surface, indicating a homogeneous and symmetric structure like the flat-sheet samples. The EDS analysis performed on the tubular PEE membranes determined that its elemental composition was similar to the flat-sheet PEE membranes.

FESEM images of the surface and cross section of a virgin CTA membrane are shown in **Figure 7**. The CTA membrane was constructed of two distinct layers (i.e., it was an asymmetric membrane: an active separating layer and an interwoven fibrous support layer. The active layer was characterized by an average thickness of 10 µm. The supporting layer was approximately

105 μm thick resulting in a total thickness of 115 μm . The CTA membrane therefore had a separating layer that was thinner than the thinnest PEE membrane studied here.

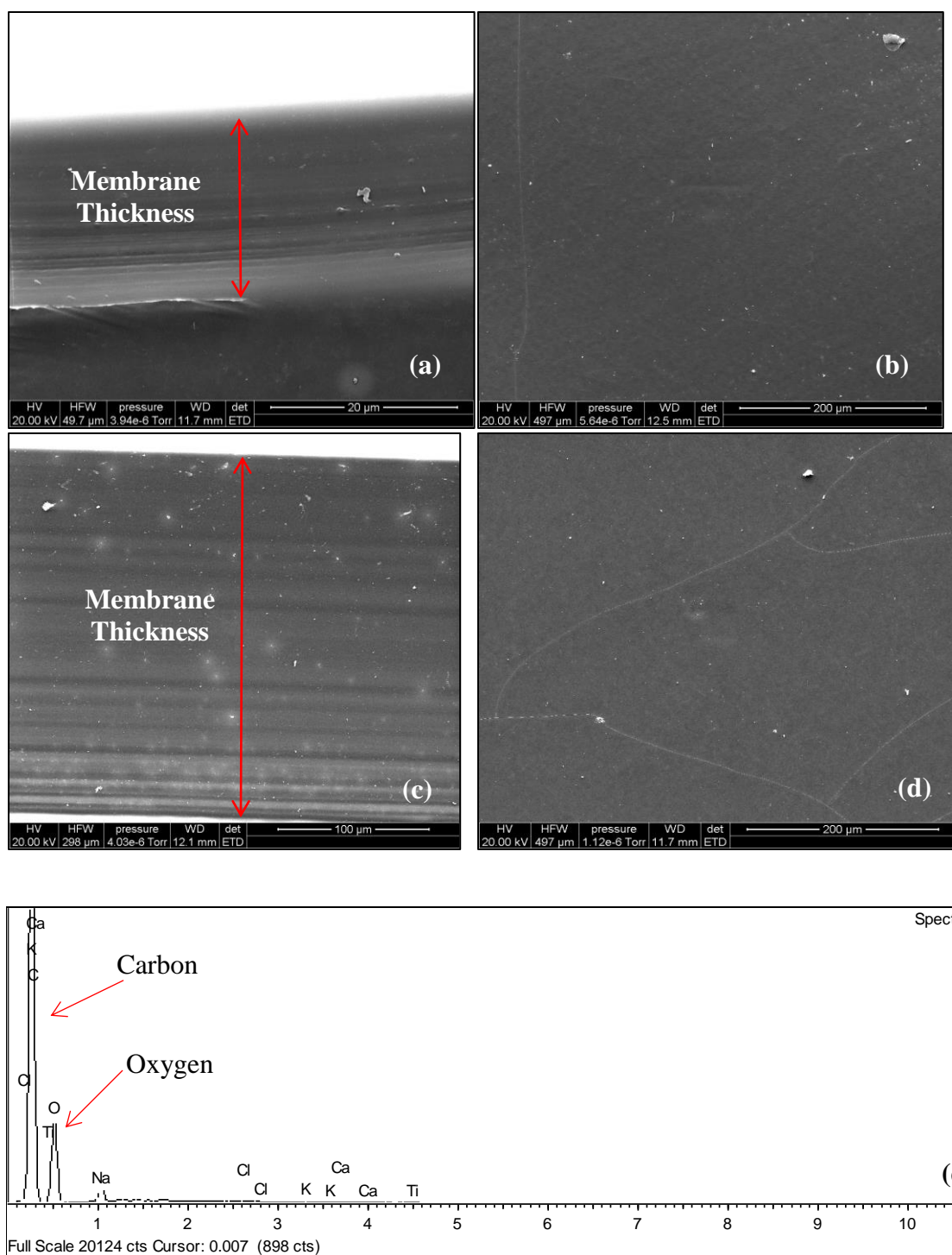


Figure 6 - Representative FESEM images of (a) cross section of 20 μm thick membrane, scale bar = 20 μm; (b) surface of 20 μm thick membrane, scale bar = 200 μm; (c) cross section of 250 μm membrane, scale bar = 250 μm, scale bar = 100 μm; and (d) surface of 250 μm thick membrane, scale bar = 200 μm; and (e) EDS analysis of virgin PEE membrane.

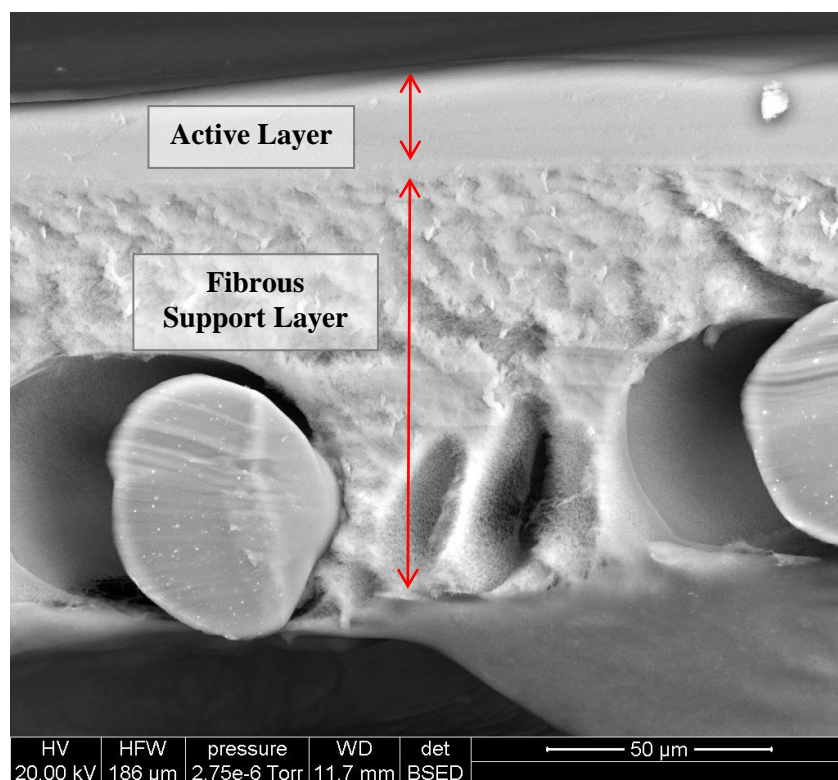


Figure 7 - FESEM image of a virgin CTA membrane used in the pervaporation experiments. The CTA membrane has an active layer thickness of 10 μm (top arrow in image), with a porous/fibrous support layer beneath the active layer (bottom arrow). The total thickness of the CTA membrane was 115 μm . The scale bar in the image reads 50 μm .

BENCH-SCALE PERVAPORATION PERFORMANCE TESTING

Relationships between Water Flux, Water Temperature, and Membrane Thickness

Water flux as a function of vapor pressure gradient (ΔVP) was measured for each flat-sheet PEE membrane thickness and the CTA membrane with the results summarized in **Figure 8**. From **Figure 8(a)**, flux generally increased with increasing ΔVP . The increase in flux due to the increase in ΔVP was more substantial for the thinner PEE membranes (thickness $\leq 50 \mu\text{m}$). From ΔVP 2,300 Pa to $\Delta VP = 12,275$ Pa the permeate flux was found to increase by approximately 150% through the 20 μm thick PEE membrane and by approximately 41% through the 50 μm thick PEE membrane. It was also found that fluxes through the CTA membrane increased with increasing ΔVP ; permeate flux increased by more than 400% over the range of ΔVP examined for the CTA membrane (**Figure 8[b]**). Water fluxes for the CTA membrane were found to be

much higher than those measured for the PEE membranes, regardless of ΔVP and/or PEE membrane thickness. For the largest ΔVP analyzed ($= 12,275$ Pa), the flux for the CTA membrane was approximately five times that for the thinnest PEE membrane ($5.65 \times 10^{-2} \text{ m}^3 \text{ m}^{-2} \text{ day}^{-1}$ and $1.19 \times 10^{-2} \text{ m}^3 \text{ m}^{-2} \text{ day}^{-1}$ for the CTA and $20\mu\text{m}$ PEE membrane, respectively). The greater water fluxes through the CTA membrane could be attributed to the thinner active layer of the CTA membrane compared to the PEE membranes. Also, the CTA membrane was characterized by a greater affinity for water relative to the PEE membrane. The flux and ΔVP were found to have a strong linear correlation, particularly for the 20 and $50\mu\text{m}$ thick PEE membranes ($R^2 = 0.99$ and 0.97 , respectively) and the CTA membrane ($R^2 = 0.98$) (**Figure 8**).

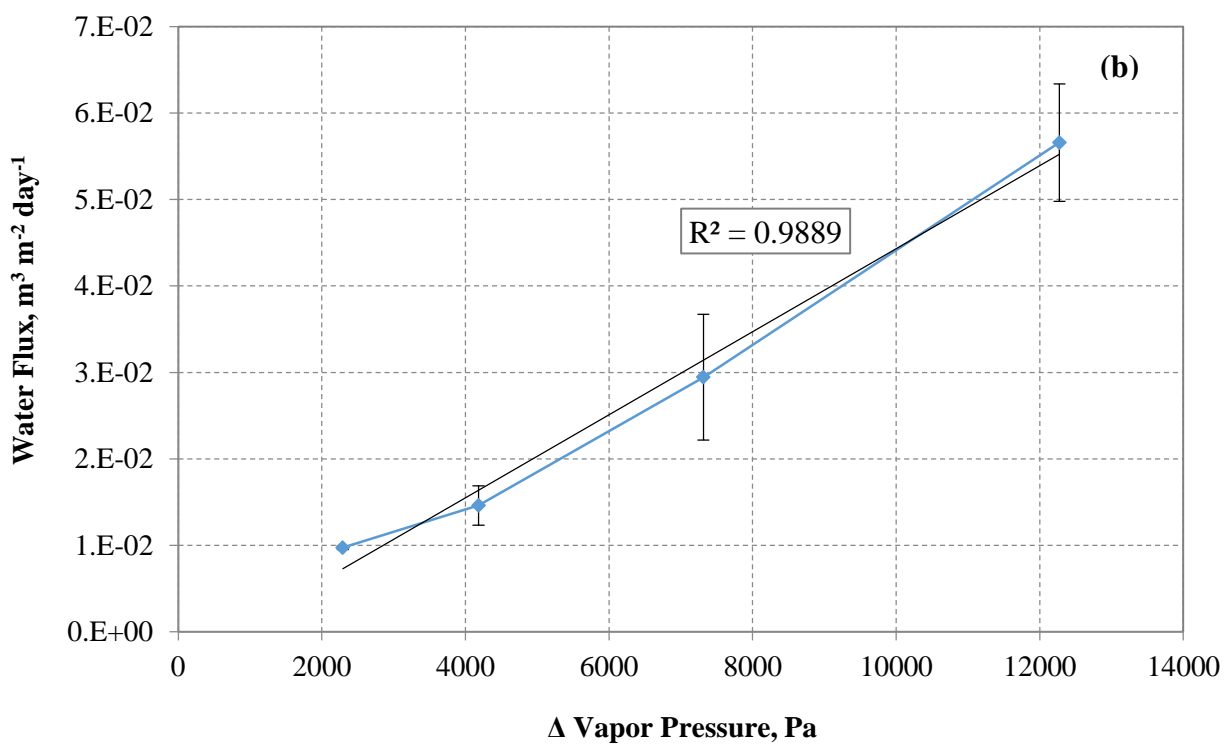
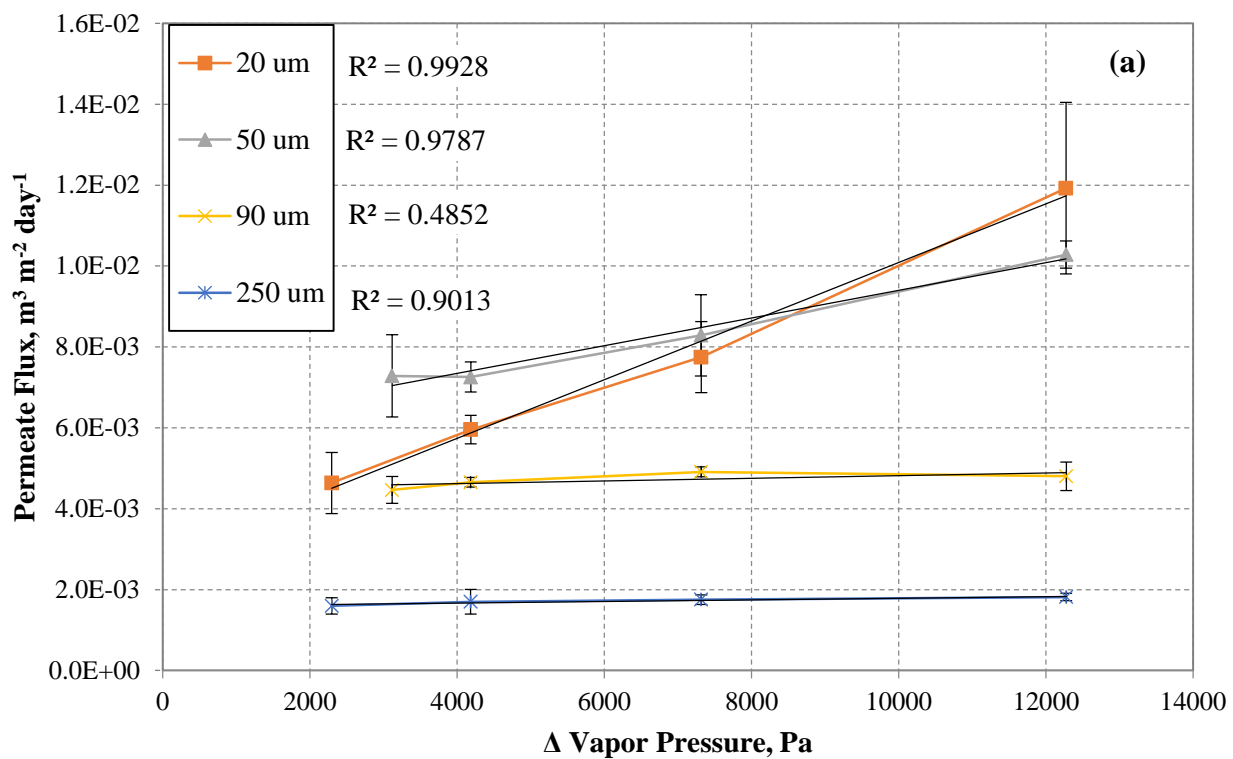


Figure 8 - Water flux as a function of the vapor pressure differential between the feed water and sweeping gas for each of the different thicknesses of the (a) flat-sheet PEE and (b) CTA membranes. The feed water used was DDW (pH = 5.5, $n = 3$).

Water fluxes for the PEE membranes were inversely proportional to membrane thickness for a given set of test conditions (**Figure 9**). The water flux through each PEE membrane and the CTA membrane was plotted in terms of the membrane thickness for each of the ΔVP values tested (**Figure 9**). The flux did appear to decrease as the membrane thickness increased, however, this was not a linear relationship ($R^2 \leq 0.37$). This non-linear relationship points to the fact that more than just membrane thickness is governing the flux; membrane chemistry and structure are likely involved as well.

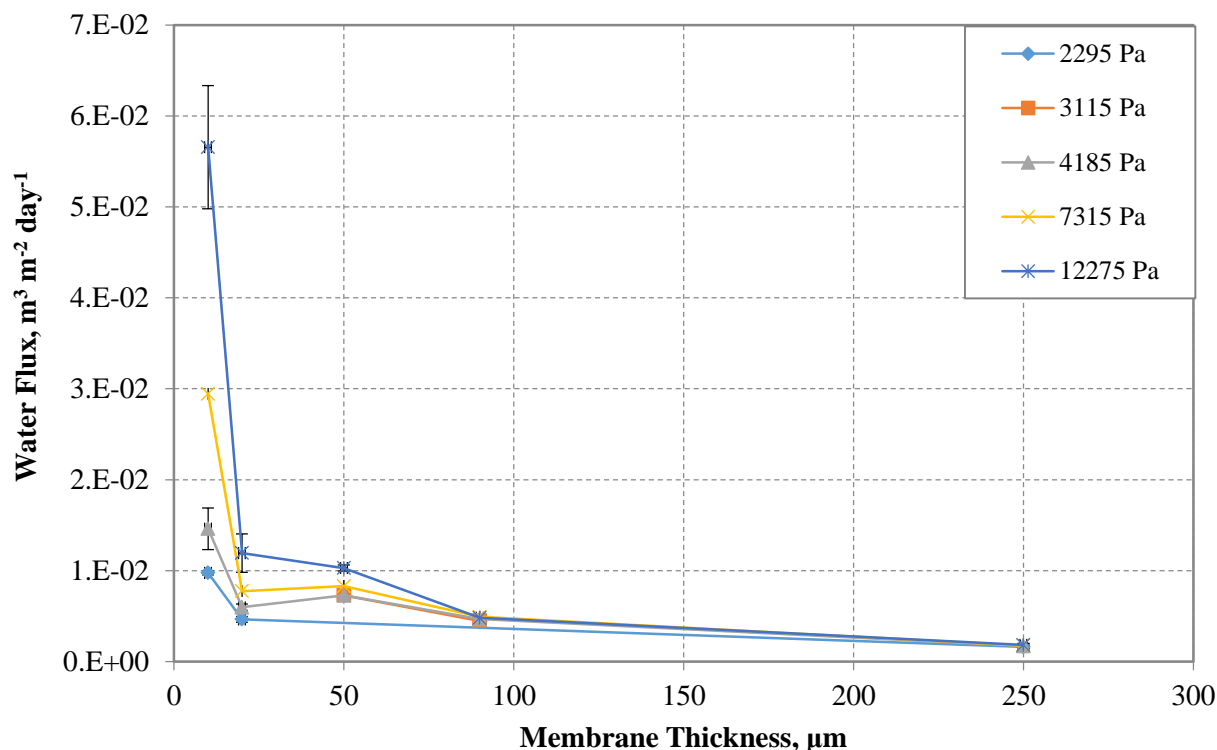


Figure 9 - Water flux versus membrane thickness for the flat-sheet PEE membranes ($l = 20, 50, 90$ and $250 \mu\text{m}$) and CTA membrane ($l = 10 \mu\text{m}$). Doubly deionized water (DDW, $\text{pH} = 5.5$) was used as the feed solution for all reported tests.

Effects of solutes on the Pervaporation Membrane Performance (Flux and Rejection)

To quantify how salinity affects the performance of pervaporation processes, water flux was measured as a function of the NaCl concentration in the feed water (a constant ΔVP of 12,275 Pa was maintained). Results from these tests are summarized in **Figure 10**. Note that the salinity of seawater is approximately 36 g L^{-1} . Therefore, a NaCl concentration of 100 g L^{-1} is

approximately three times that of seawater and approximates that commonly found in produced waters generated from the Marcellus Shale and other formations [60]. From **Figure 10[a]**, there was a decrease in water flux as the salinity of the feed water increased, particularly for the thinnest ($l = 20\ \mu\text{m}$) PEE membrane. Flux decreased by 800% for the $20\ \mu\text{m}$ thick PEE membrane and by 50% for the $250\ \mu\text{m}$ thick PEE membrane. Linear regression of each membrane thickness showed that there was a strong linear correlation between flux and feed water salinity for either membrane thickness ($R^2 = 0.887$ and 0.686 for the 20 and $250\ \mu\text{m}$ PEE membranes, respectively). The water flux for the CTA membrane also decreased with increasing salinity (**Figure 10[b]**). A total decrease in water flux of 40% was determined for the CTA membrane as the salt concentration increased from 10 to $100\ \text{g L}^{-1}$ ($R^2 = 0.970$).

Beyond the decreased vapor pressure due to increased salt concentration, other possible causes for the decrease in water flux (**Figure 10**) include concentration polarization and the loss of water adsorption by the membrane due to the decreased thermodynamic activity of the water from the increased NaCl concentration. Sodium chloride is highly soluble ($\sim 363\ \text{g L}^{-1}$ at $T = 50^\circ\text{C}$ and $P = 101.325\ \text{kPa}$ [61]). Therefore it is not likely that the salt precipitated from solution, subsequently forming a scale on the membrane surface, under the conditions tested here. However, as water permeated through the PEE and CTA membranes the local ion concentrations at the membrane surface will be elevated relative to that in the bulk solution. This is referred to as concentration polarization [62]. This can lead to a decrease in flux as the increased salt concentrations lead to a decrease in vapor pressure which decreases the driving force for pervaporation membranes. The increased salt concentration in the feed water results in decreased thermodynamic activity of the water which then leads to decreased solvent (water) uptake by the membrane, as observed during the flat-sheet swelling experiments. The decrease in water uptake by the polymer could possibly lead to decreased flux.

One way to increase flux through membranes without changing the membrane thickness or environmental conditions, is through the use of spacers. Spacers create/enhance turbulence at the membrane-solution interface [63-65]. This increase in shear forces reduces the thickness of the concentration polarization boundary layer and other deposits on the membrane surface. In this way, spacers may be used to mitigate the formation of cake structures and/or the thickness of concentration polarization layers on salt rejecting membrane surfaces. Bench-scale tests were

therefore used to evaluate what, if any, impact inclusion of feed spacers may have on the performance of the flat-shear PEE and CTA membranes.

Water flux data for the 20 μm thick PEE membranes with and without spacers are given in **Figure 11**. Here, water increased by 590% when spacers were included and the cross flow velocity of the sweeping gas remained constant (**Figure 11**). It increased by a full order of magnitude when the cross flow velocity of the sweeping gas was increased from 0.075 to 0.170 m sec^{-1} . The increase in water flux for the PEE membrane was attributed to enhanced turbulence at the membrane surface resulting in a reduction in the concentration boundary layer. The specific mechanism(s) by which the flux was improved by the spacer remains poorly understood. Water flux through the CTA membranes (**not shown**) was found to essentially remain the same with or without the use of spacers (change in performance of 3.9%).

Experiments were also performed using more complex feed solutions: the Dutch Creek CBM water (**Table 4**) and the two conventional produced water samples (**Table 5**). The produced water samples were included in these experiments to examine how the PEE and CTA membranes performed treating representative produced waters. Since these produced waters contain a variety of salt species, and in the case of the produced waters some organic matter, membrane fouling by means of cake formation had more potential to be an issue. A constant $\Delta VP = 12,275 \text{ Pa}$ was used for all experiments ($T = 50^\circ\text{C}$, RH of sweeping gas = 2%). Average water fluxes for the two membranes treating the three produced water samples are given in Figure 12. Water fluxes through the PEE membrane (**Figure 12[a]**) were 29.8 -40.5% greater for the CBM water (1.5 g L^{-1}) than that of the NaCl solution (100 g L^{-1}) and the PW1 and PW2 samples (60.05 and 77.38 g L^{-1} , respectively). Due to the complexities of the produced water samples, accurate vapor pressure values could not be determined. So it was not possible to determine if changes in water flux for the different produced water samples were due to differences in ΔVP . However, as determined during the water adsorption experiments, the PEE membranes were shown to uptake less water as the salinity of the water increased. Since the water fluxes of the produced waters and NaCl solution were less than the fluxes of the CBM water through the PEE membrane, osmotic de-swelling could have been occurring during these experiments. Water fluxes through the CTA membranes (**Figure 12[b]**) were very similar for all produced water samples used

(PW1, PW2, and CBM waters were all within 5% of one another), but about 25% lower for the NaCl feed solution.

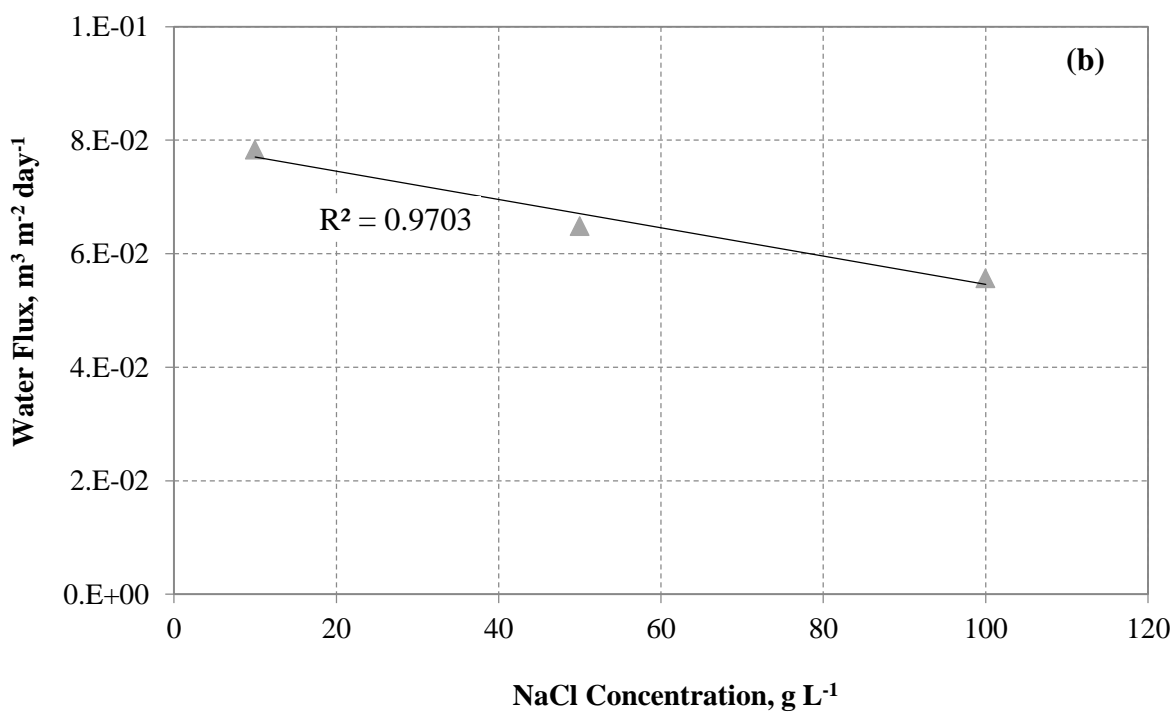
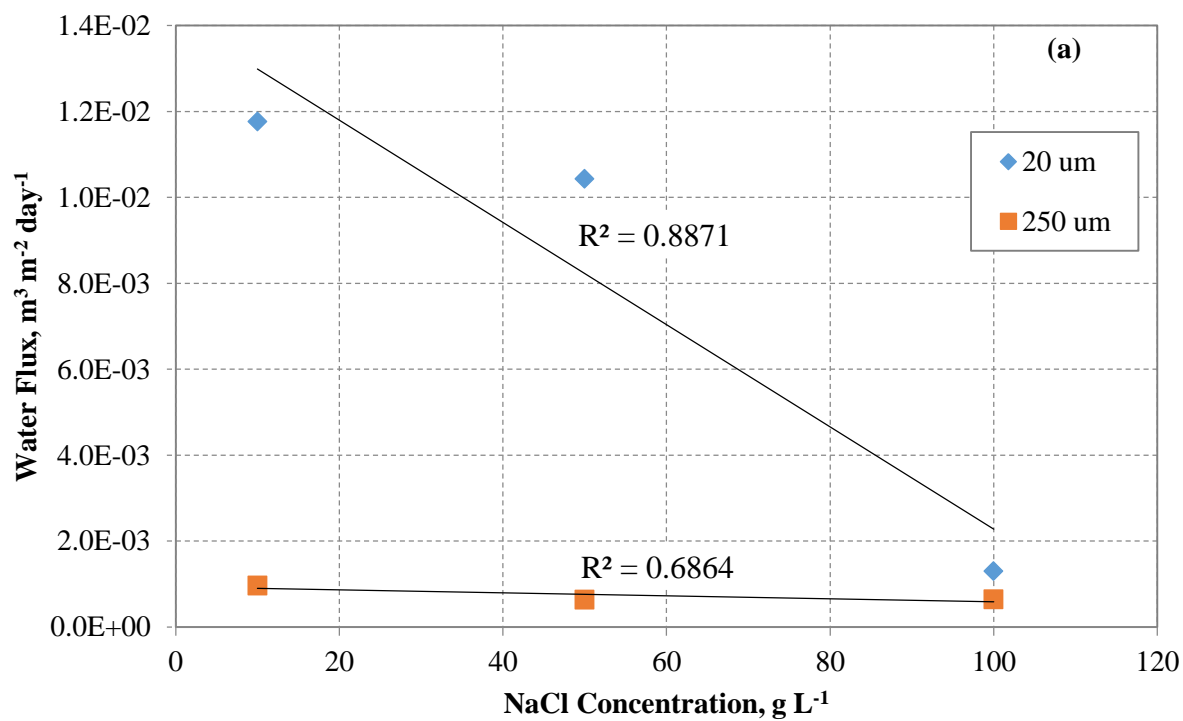


Figure 10 - Water flux as a function of sodium chloride (NaCl) concentration for the (a) 20 and 250 μm thick PEE membranes and the (b) CTA membrane ($\text{pH} = 5.5$, $\Delta VP = 12,275 \text{ Pa}$, $n = 2$).

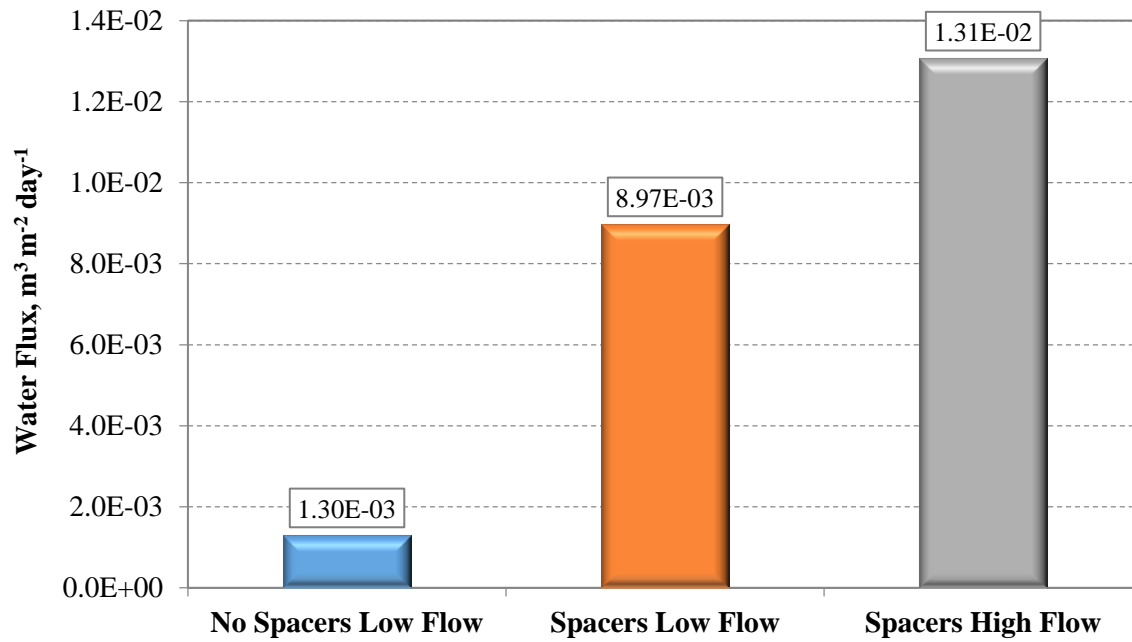


Figure 11 - Water flux through the flat-sheet PEE membrane in the presence and absence of feed spacers ($l = 20 \mu\text{m}$, low air flow = 0.075 m sec^{-1} , high air flow = 0.170 m sec^{-1} , $[\text{NaCl}] = 100 \text{ g L}^{-1}$, $\Delta VP = 12,275 \text{ Pa}$, $n = 2$).

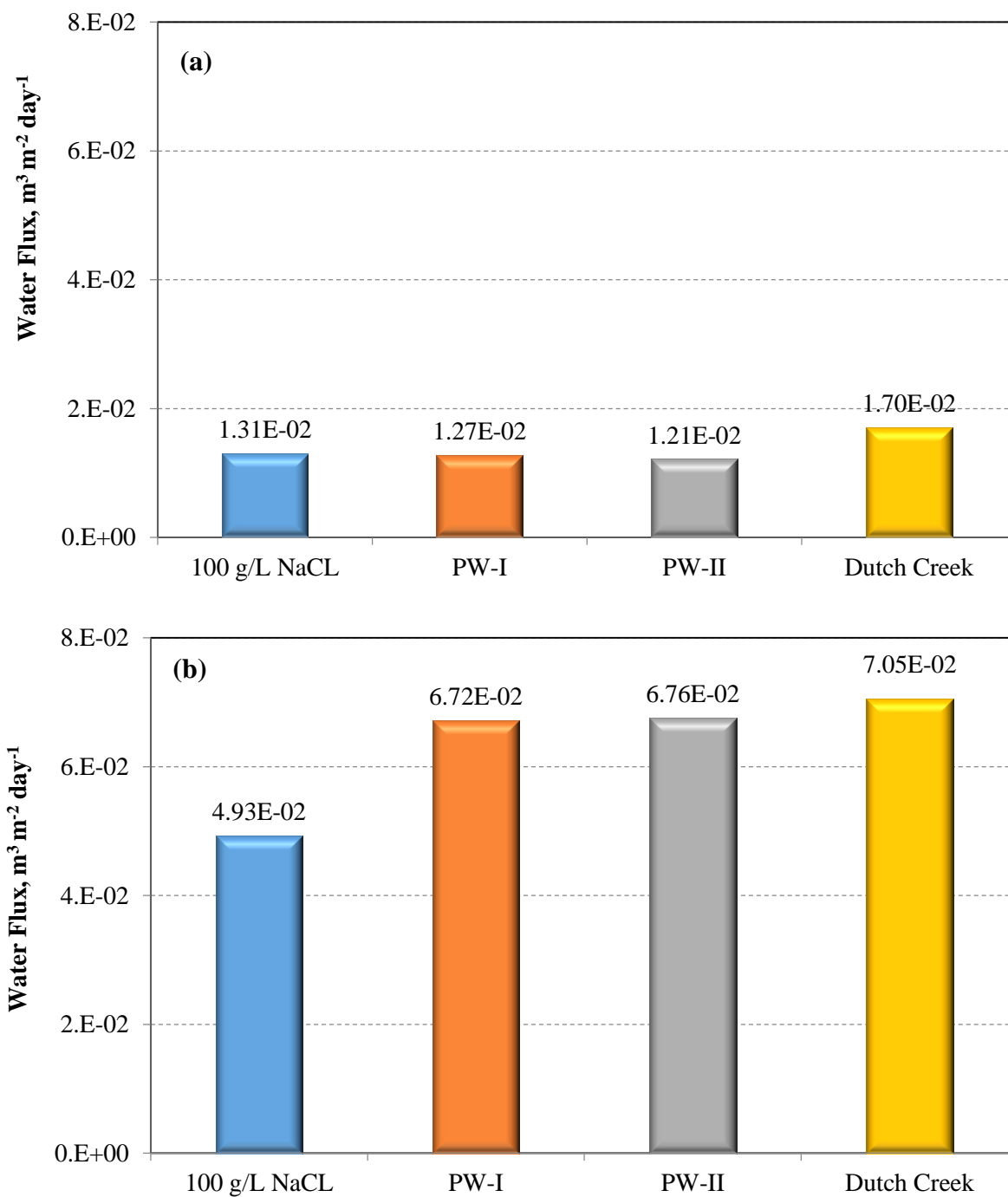


Figure 12 - Water flux for (a) 20 μm thick PEE membrane and (b) CTA membrane when using produced waters as feed waters in the bench-scale pervaporation experiments ($\Delta VP = 12,275$ Pa, $T = 50^\circ\text{C}$, RH of sweeping gas = 2%, $n = 2$).

PERFORMANCE ASSESSMENT OF PERVAPORATION IRRIGATION

Laboratory and field-scale experiments were done to evaluate the performance of the tubular pervaporation membranes when buried in different soils. Soil box tests were designed to establish baseline flux and salt rejection data for the membranes. Grow box tests were done to elucidate the impact that vegetation will have on water flux across the pervaporation membranes. Finally, field tests were carried out to examine the impact(s) that environmental variable have on process performance. The main goals of these tests were as follows:

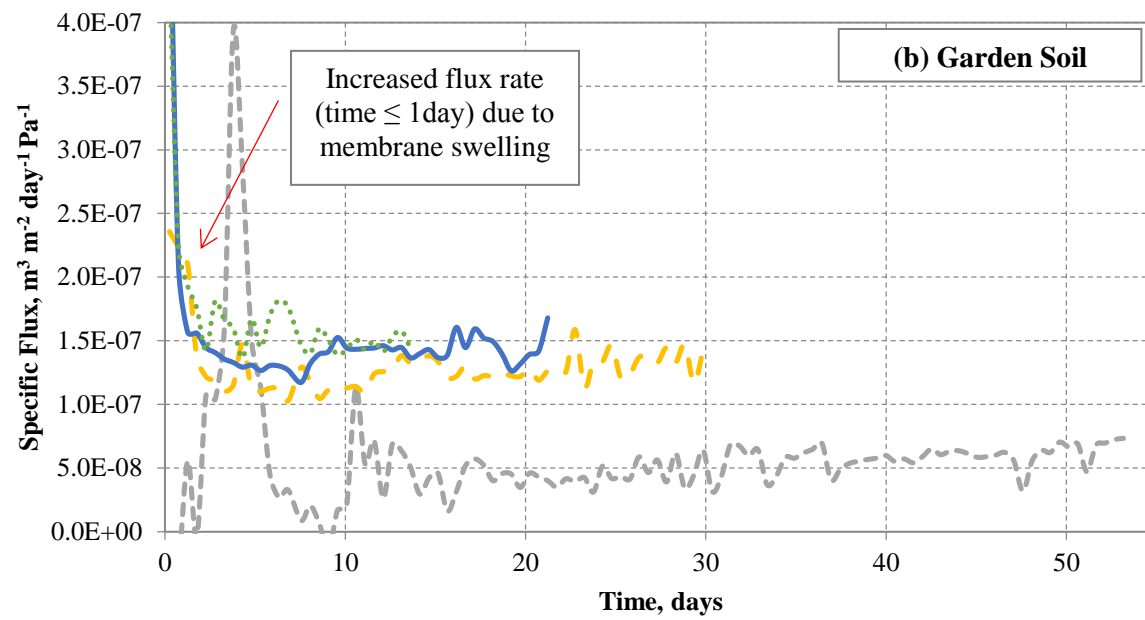
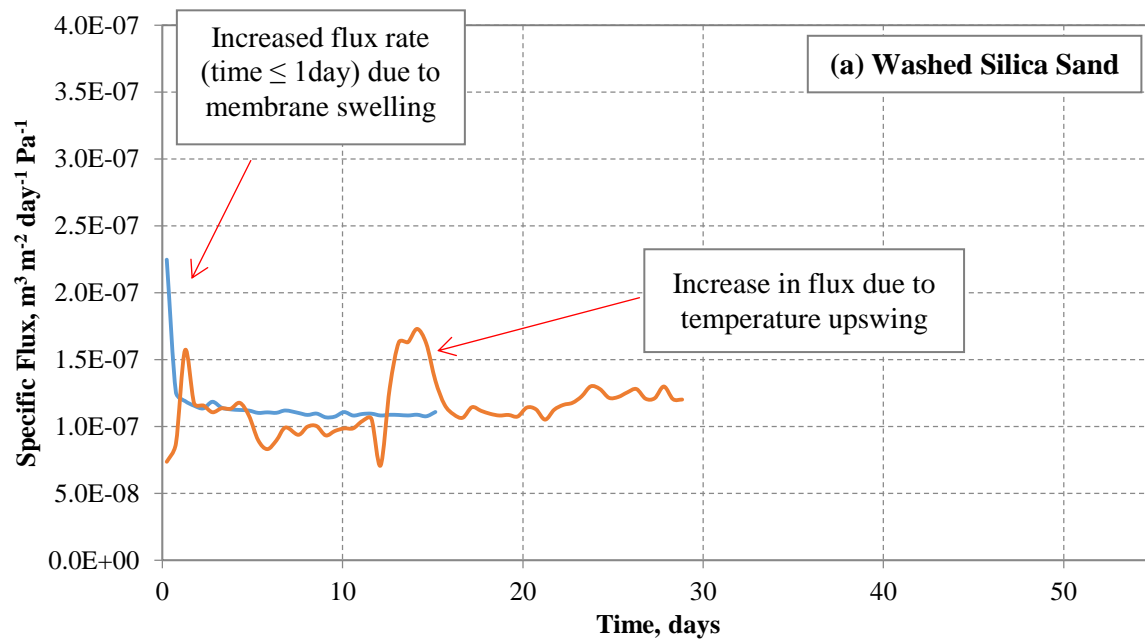
1. Acquire baseline performance (flux, salt rejection) for the pervaporation membranes when buried in soil and as a function of environmental conditions. Variables that were accounted for in these tests included soil type, soil moisture, relative humidity of the surrounding atmosphere, and water uptake by vegetation (alfalfa).
2. Evaluate how performance varied over time as a result of increasing salinity within the tubular pervaporation membrane.
3. Assess changes in feed water quality over time and qualitatively determine if membrane fouling had occurred and its impact on membrane performance.

Soil box experiments – Effect of membrane characteristics, environmental conditions on the membrane performance

The membrane used in the soil box experiments was the tubular PEE membrane ($l_{average} = 400$ to $650\ \mu\text{m}$). Test conditions used in these tests are summarized in **Table 3**. Specific water flux values as a function of time for the tubular PEE membrane buried in the different soil types (washed silica sand [a], garden soil [b] and clay loam soil [c]) are shown in **Figure 13**. A summary of the average water fluxes, temperatures, relative humidity values and soil moisture contents for each of the soil box tests is given in **Table 9**. The water fluxes through the PEE irrigation tubing were elevated at the beginning of each test ($t < 1$ day), relative to those values measured in the remainder of the test, due to adsorption of water by the membrane material. At $t > 1$ day, the water flux reached a relatively stable value for the remainder of each experiment. The permeate flux curve for soil box test 3 was the only one that did not follow the same trend as the other tests performed. This was because the garden soil placed in the soil box at the beginning of soil box test 3 was very moist (initial soil moisture nearest pervaporation tubing = 11 % and RH at soil surface = 76%, as opposed to soil moisture = 2 - 6 % and RH = 4 - 36% at

the startup of the other experiments), so the driving force ($p_{io} - p_{il}$) for pervaporation was very low (initial ΔVP was around 512 Pa). As test 3 progressed, the sweeping gas dehydrated the soil and the flux increased (**Figure 13[b]**) until reaching a similar flux as measured in the other soils. The slight variations in flux that were measured in each of the tests were due to changes in room, which affects the ΔVP . Changes in the mass of water in the feed tank resulting from drawing samples from the sample line and the addition of more water to the feed tank contributed to fluctuations in the flux data. The water flux (see **Table 9**) for each test plateaued at approximately $1.74 - 5.74 \times 10^{-4} \text{ m}^3 \text{ m}^{-2} \text{ day}^{-1}$. The fluxes through the PEE tubing were an order of magnitude less than the fluxes observed through the 20 μm flat-sheet PEE membrane at similar ΔVP values (permeate flux = $5.96 \times 10^{-3} \text{ m}^3 \text{ m}^{-2} \text{ day}^{-1}$ at $\Delta VP = 4185 \text{ kPa}$).

The effect of recycling the feed (Dutch Creek CBM water, **Table 4**) through the PEE membrane on the specific permeate flux through the PEE membranes was also studied (**Figure 14**). Tests 7 and 8 were conducted with two different PEE membrane samples with the same thickness (650 μm). Even though recycling the feed only provided a small improvement to the water flux ($1.67 \times 10^{-7} \text{ m}^3 \text{ m}^{-2} \text{ day}^{-1}$ with recycle and $1.60 \times 10^{-7} \text{ m}^3 \text{ m}^{-2} \text{ day}^{-1}$ without recycle), it was decided to recycle the feed for the subsequent tests (Test 9 and Grow Box test) as we felt the feed recycling provides better mixing within the tubular membrane. This enhanced mixing reduces the thickness of the concentration polarization boundary layer and may scour away any deposits that have formed on the membrane surface. This conclusion was based on our observations that were made with the flat-sheet PEE membranes and feed channel spacers. The data shown in **Figure 14** demonstrates the improvement in flux obtained by using a tubular CTA membrane relative to that measured for the PEE membrane. The specific flux is about 6 times higher for the CTA than the flux that was measured for the PEE membrane (Test 8) under the same environmental conditions and using the same feed solution. The higher water flux that was measured for the CTA membrane agrees with our results that were obtained for the flat-sheet PEE and CTA membranes. It is attributed to the thinner separating layer for the CTA membrane (10 μm versus 650 μm) and the CTA's greater affinity for water.



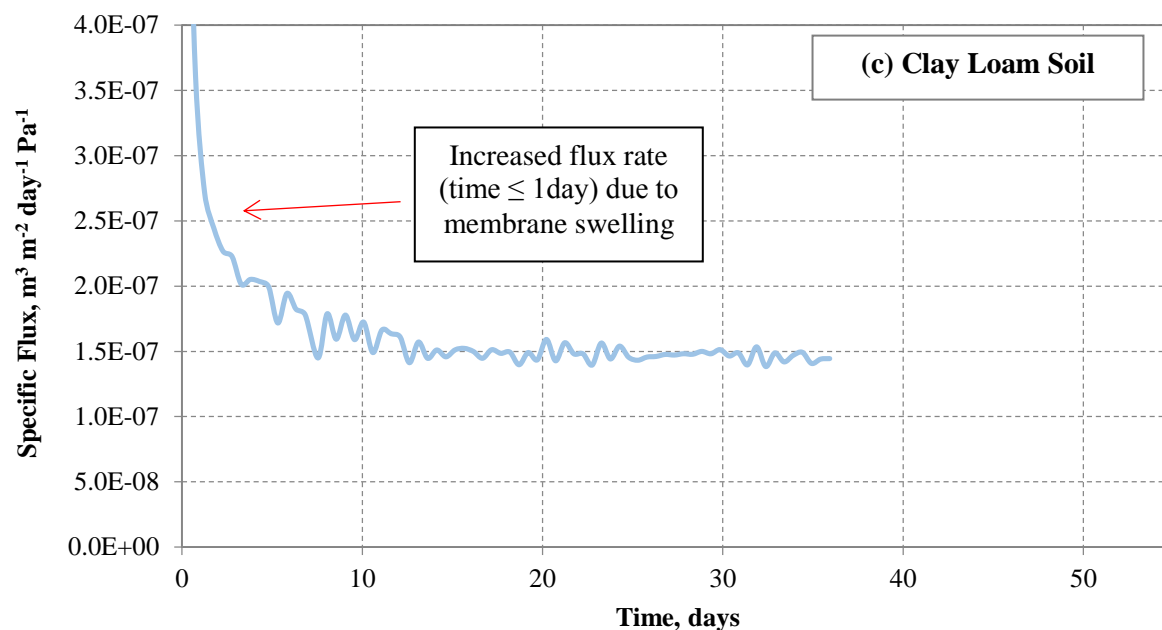


Figure 13 - Specific flux for the tubular PEE membrane when treating CBM water in the soil box apparatus. Each plot displays water fluxes through the tubing when surrounded by different types of soil: tests 1 and 2 used washed silica sand (a); tests 3-6 used garden soil (b), and test 7 used clay loam soil (c). Environmental/membrane conditions for each test are summarized in Table 3.

The average specific flux values for the tubular PEE membranes are summarized for each soil type in **Figure 15**. Values in **Figure 15** were obtained using PEE membranes having a thickness of 650 μm and using CBM produced water as the feed water. The specific fluxes through the tubing when surrounded by garden soil and clay loam soil were essentially the same (1.91% difference) and were found to be about 41% greater than that measured for the washed silica sand. One explanation for this is that the garden soil and clay loam soil have a greater capacity for holding moisture than the sand (typical saturation moisture contents are 0.37, 0.46 and 0.47 for sand, loam and clay loam, respectively). In essence the sand is less capable of drawing moisture away from the tubing than the other two soil types. This in turn results in higher moisture contents in the immediate vicinity of the membrane. This reduces the ΔVP across the membrane and hence lower water flux.

Table 8 - Summary of average water fluxes and environmental variables for the soil box tests.

| Test # | Soil | Membrane Thickness, μm | Flux, $\text{m}^3 \text{m}^{-2} \text{day}^{-1}$ | Specific Flux, $\text{m}^3 \text{m}^{-2} \text{day}^{-1} \text{Pa}^{-1}$ | Vapor Pressure Gradient, Pa | Relative Humidity in Head Space, % | Soil Moisture, $\text{m}^3 \text{m}^{-3}$ |
|--------|--------------------|-----------------------------------|--|--|-----------------------------|------------------------------------|---|
| 1 | Washed Silica Sand | 650 | $4.60 \times 10^{-4} \pm 1.47 \times 10^{-5}$ | $1.11 \times 10^{-7} \pm 3.49 \times 10^{-9}$ | $4,056 \pm 8.09$ | 1.67 ± 0.27 | 0.05 ± 0.01 |
| 2 | Washed Silica Sand | 650 | $3.90 \times 10^{-4} \pm 6.66 \times 10^{-5}$ | $1.16 \times 10^{-7} \pm 2.07 \times 10^{-8}$ | 3378 ± 140.8 | 1.59 ± 0.61 | 0.05 |
| 3 | Garden Soil | 650 | $1.74 \times 10^{-4} \pm 1.01 \times 10^{-4}$ | $5.88 \times 10^{-8} \pm 5.12 \times 10^{-8}$ | 3055 ± 797 | 21.07 ± 20.50 | 0.07 ± 0.04 |
| 4 | Garden Soil | 650 | $4.48 \times 10^{-4} \pm 7.51 \times 10^{-5}$ | $1.27 \times 10^{-7} \pm 2.07 \times 10^{-8}$ | 3755 ± 69.6 | 4.56 ± 1.63 | 0.04 ± 0.02 |
| 5 | Garden Soil | 500 | $5.74 \times 10^{-4} \pm 4.55 \times 10^{-5}$ | $1.41 \times 10^{-7} \pm 1.21 \times 10^{-8}$ | 4086 ± 186.1 | 3.06 ± 1.27 | 0.02 |
| 6 | Garden Soil | 400 | $5.53 \times 10^{-4} \pm 6.79 \times 10^{-5}$ | $1.57 \times 10^{-7} \pm 1.89 \times 10^{-8}$ | 3541 ± 60.7 | 11.10 ± 2.41 | 0.02 |
| 7 | Clay Loam | 650 | $3.89 \times 10^{-4} \pm 4.90 \times 10^{-5}$ | $1.60 \times 10^{-7} \pm 2.75 \times 10^{-8}$ | 2425 ± 176.4 | 11.01 ± 4.62 | 0.09 ± 0.02 |
| 8 | Clay Loam | 650 | $4.53 \times 10^{-4} \pm 1.42 \times 10^{-4}$ | $1.67 \times 10^{-7} \pm 4.93 \times 10^{-8}$ | 2701 ± 67.3 | 14.64 ± 2.1 | 0.08 ± 0.02 |
| 9 | Clay Loam | 10 | $2.74 \times 10^{-3} \pm 4.53 \times 10^{-3}$ | $9.91 \times 10^{-7} \pm 1.64 \times 10^{-8}$ | 2754 ± 72.5 | 12.14 ± 0.59 | 0.12 ± 0.03 |

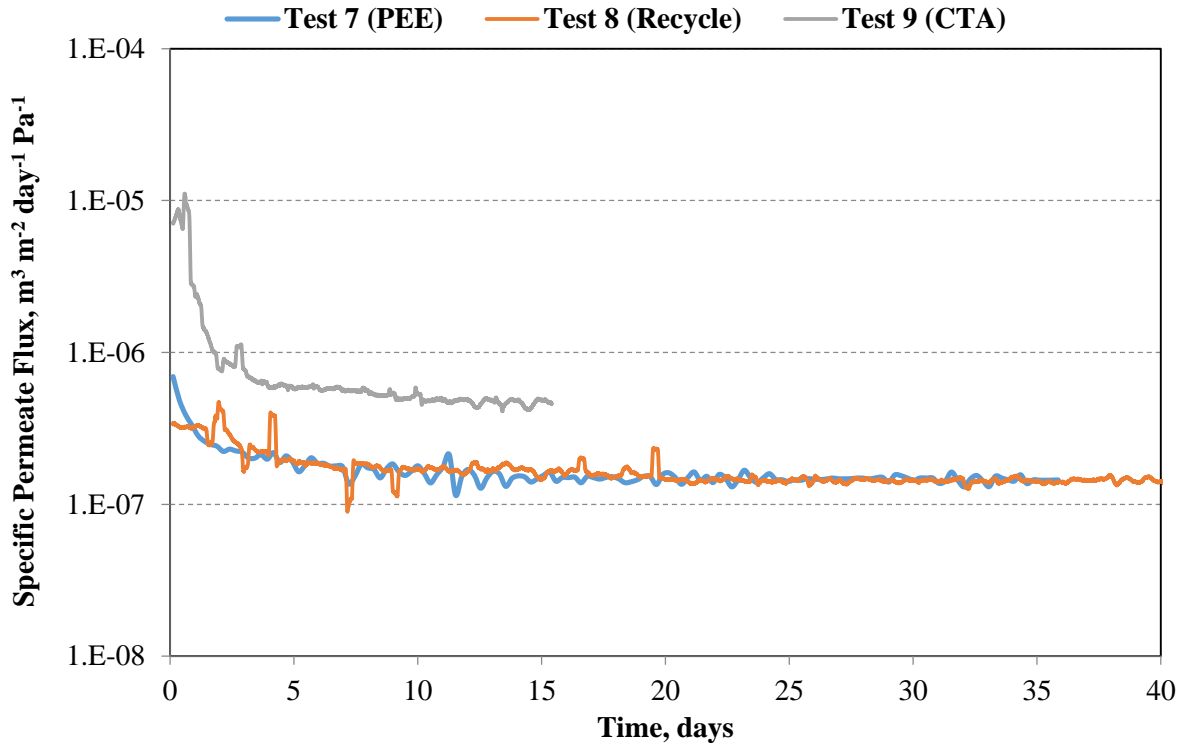


Figure 14 - Specific flux for the tubular PEE (Tests 7 and 8) and CTA (Test 9) membranes when treating CBM produced water in the soil box test apparatus (soil = clay loam, PEE thickness = 650 μm).

Water flux through different thicknesses of the PEE pervaporation tubing were also examined. The average specific flux through the 400, 500 and 650 μm thick PEE pervaporation tubes is shown in **Figure 16**. Specific flux increased as membrane thickness decreased. This agreed with theoretical predictions for water flux and with the results for the flat-sheet PEE membranes. A strong linear correlation was found between the specific flux and membrane thickness ($R^2 = 0.994$).

The conductivity and pH of the feed water, as well as the conductivity of the reject water within the pervaporation tubing, were periodically measured during each experiment and the results for a representative test (Test 7) is shown in **Figure 17**. Similar trends were observed for all the nine soil box tests as well as the grow box test. The conductivity and pH were both determined to increase during each of the experiments. This was expected to happen since the system was operating in a dead-end configuration and the concentration of salts in the feed

tank/pervaporation tubing increased as water was filtered through the membrane. Since the main constituent in the CBM produced water is NaHCO_3 , it was expected that the pH would also increase as the overall salt concentration increases. The conductivity of the reject water was, generally, found to increase at a faster rate than the conductivity of the feed water. This was likely due to a lack of back transfer of salt up the feed line during operation. The water fluxes remained steady in all of these experiments even when salt crystals were forming on the membrane surface (feed side). This is encouraging because it means the pervaporation tubing shows the potential to exhibit consistent membrane performance (flux) for long-term use in an irrigation system.

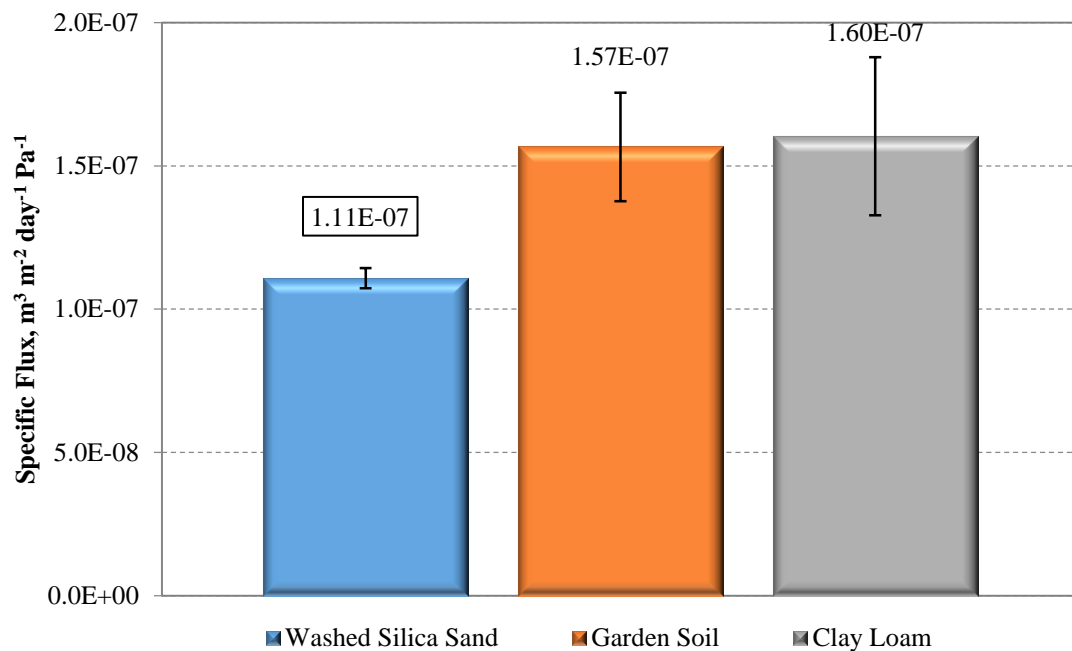


Figure 15 - Average specific flux ($\text{m}^3 \text{m}^{-2} \text{day}^{-1} \text{Pa}^{-1}$) through the PEE pervaporation tubing when surrounded by different soil types: washed silica sand (blue column); garden soil (red column); and clay loam soil (green column). The feed water used for each test was CBM water; the membrane thickness used for each sample was 650 μm .

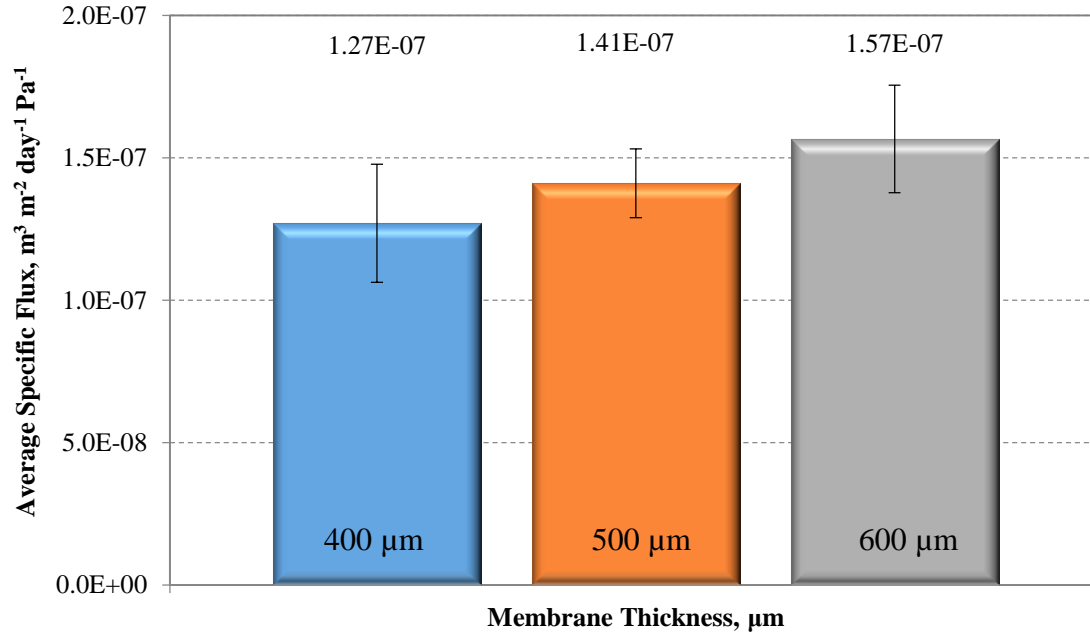


Figure 16 - Average specific flux ($\text{m}^3 \text{m}^{-2} \text{day}^{-1} \text{Pa}^{-1}$) for each thickness of the tubular PEE membrane when treating CBM produced water (soil = garden soil). The 400 μm thick membrane (56 g m^{-1}) is represented by the blue column, the 500 μm thick membrane (70 g m^{-1}) is represented by the red column, and the 650 μm thick membrane (90 g m^{-1}) is represented by the green column.

Permeate produced by the membrane was in vapor form, and subsequently may, or may not, be retained by the soil. Furthermore, the long duration of the soil box tests made using a condensing vessel impractical. Thus, it was not possible to collect permeate samples to calculate salt rejection for the different membrane systems. Since the permeate concentration could not be directly measured, the rejection of the pervaporation tubing had to be calculated theoretically using the known feed and reject salt concentrations. Salt rejection was estimated by fitting the theoretical and actual salt concentrations in the reject stream using rejection efficiency (r) as the fitting parameter ($r = 1 - C_p/C_f$). The theoretical salt concentration in the reject stream was determined using **Equation 7**.

$$C_r = CF * C_f \quad (7)$$

where CF is the concentration factor (unitless); C_r is the concentration of the reject water inside the pervaporation tubing measured as a conductivity (mS cm^{-1}); and C_f is the concentration of the feed water measured as a conductivity (mS cm^{-1})

The calculated (see **Eq. 7**) salt concentration in the reject water for each soil box test was plotted against the measured reject conductivity (measured in terms of conductivity) values and the results are presented in **Figure 18**. The theoretical concentration and actual rejection concentration agreed in that they were both found to increase as each test progressed. Regression analysis of each of the different data sets shown in **Figure 18** confirmed that the calculated and measured values are in good agreement with the majority of the tests showing $R^2 \geq 0.98$. The goodness of fit (R^2 values) for these results supports our assumption of 100% salt rejection by the pervaporation membrane. Actual salt concentrations in the reject stream were consistently equal to or greater than the theoretical values indicating that the assumption of 100% rejection efficiency was sound. Additionally, the theoretical assessment of rejection agrees with the rejection efficiencies for salts that were measured for the flat-sheet pervaporation membranes.

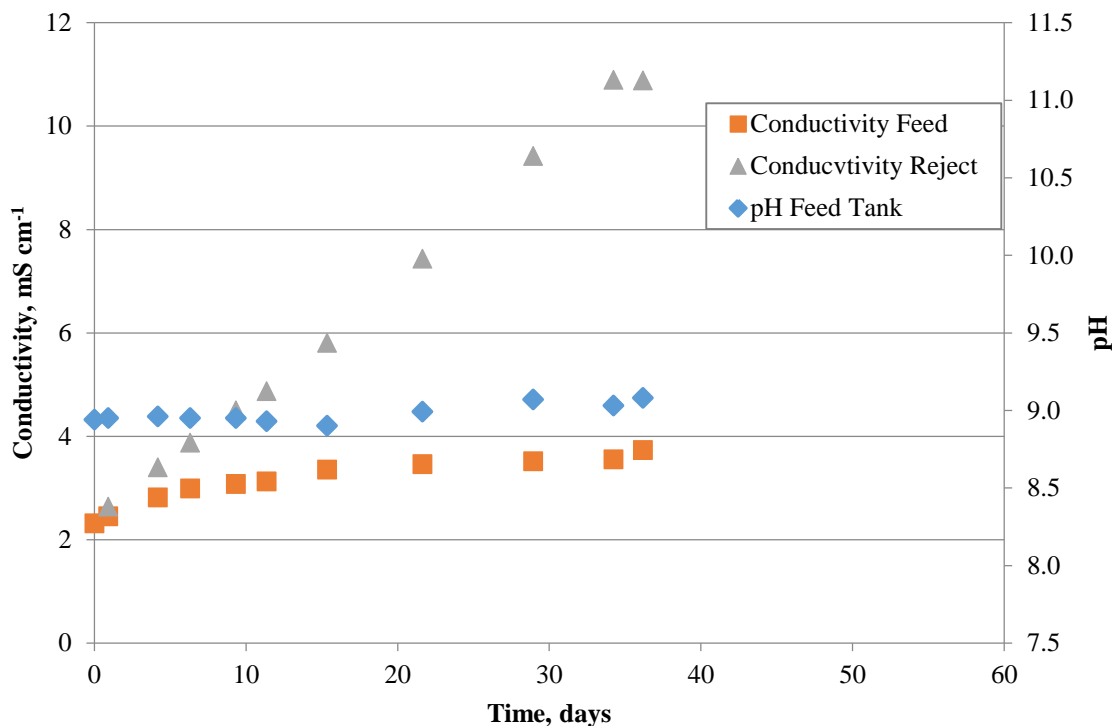


Figure 17 - Conductivity of the CBM feed and reject streams for the tubular PEE pervaporation membrane during soil box testing. The pH of CBM feed water is also reported.

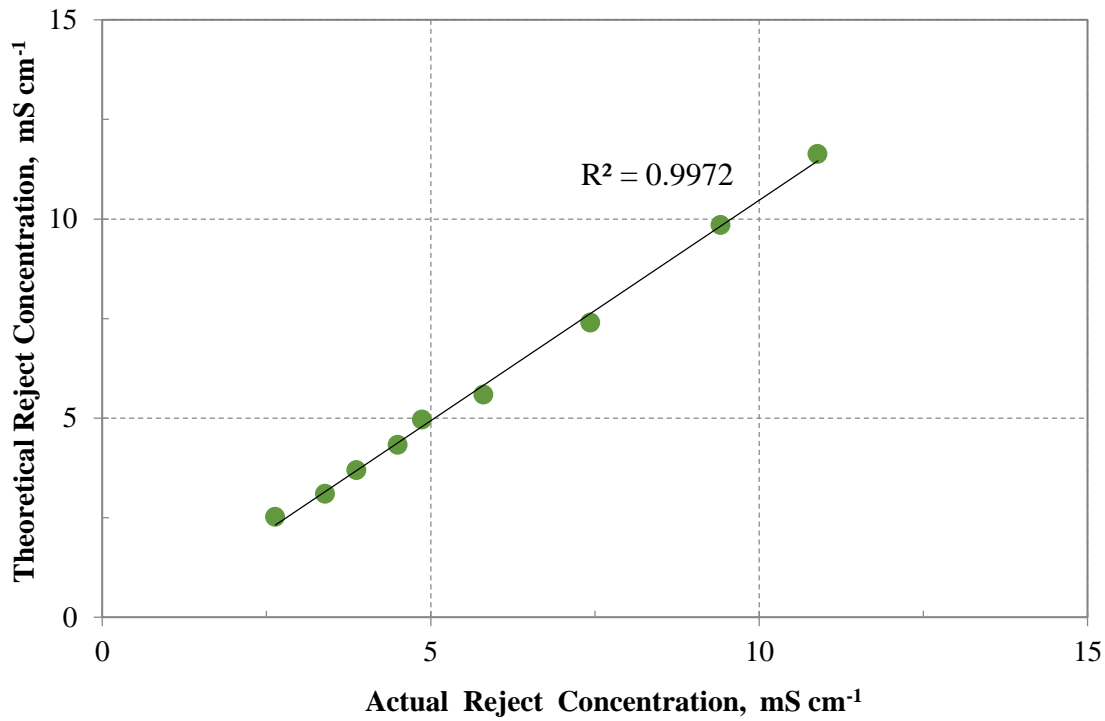


Figure 18 - Theoretical (y-axis) vs actual (x-axis) conductivity (mS cm⁻¹) of the reject water within the tubular PEE membrane during soil box Test 7.

Grow box assessment of pervaporation irrigation performance

The effect of adding plants and their subsequent water demand on the water fluxes is depicted in **Figure 21**. Plants need water for their growth which they draw from the soil and hence the soil becomes dry, decreasing the vapor pressure within the soil. This in turn aids in maintaining a high $\Delta V P$ across the pervaporation membranes. Soil box experiment 9 and the grow box experiments employed the tubular CTA membrane. This membrane was selected for study in the grow box tests because of its superior flux properties relative to the PEE membrane. The feed used in the grow box experiments is a synthetic produced water having an initial TDS concentration = 2,000 mg/L. The soil used was garden top soil. The porosity of the soil was about 31%. An important difference between the soil and grow box experiments was that the humidity was not controlled for the grow box experiments as it was open to the atmosphere. This difference can be observed in **Figure 19**, with the grow box now open to temperature and humidity variations due to the atmosphere around as well as the heat given out by the grow light, we see a diurnal trend for the flux rates. It is high during the day due to the increased temperature

(when the light is on) and low during the night (when the light is off). Another important observation from the grow box experiments is that the plants that were planted farthest from the pervaporation tube expressed severe drought stress and subsequently died as the experiment progressed (**Figure 20**). This could be due to the fact that the single tube does not provide enough flux to sustain all the plants. It could also be due to the fact that the soil is not very good at wicking moisture away from the tubes and spread it across the entire soil profile (poor hydraulic conductivity of the soil). The variation in the grow box soil volumetric moisture [m^3/m^3] immediately next to the PV tube as well as at a farther spatial location is depicted in **Figure 21**. **Figure 21[a]** depicts the variation in volumetric soil moisture content at the same depth as the buried tube. Considering an x-y slice, we see that the volumetric moisture content is much higher right next to the tube (0.20 – 0.35) compared to a location about 9 inches farther from the center in the same x-y plane (0.11 – 0.14). **Figure 21[b]** depicts a similar variation in volumetric moisture content in the x-y plane but at a different z co-ordinate. The x-y slice is taken about 9 inches directly above where the tube is buried.

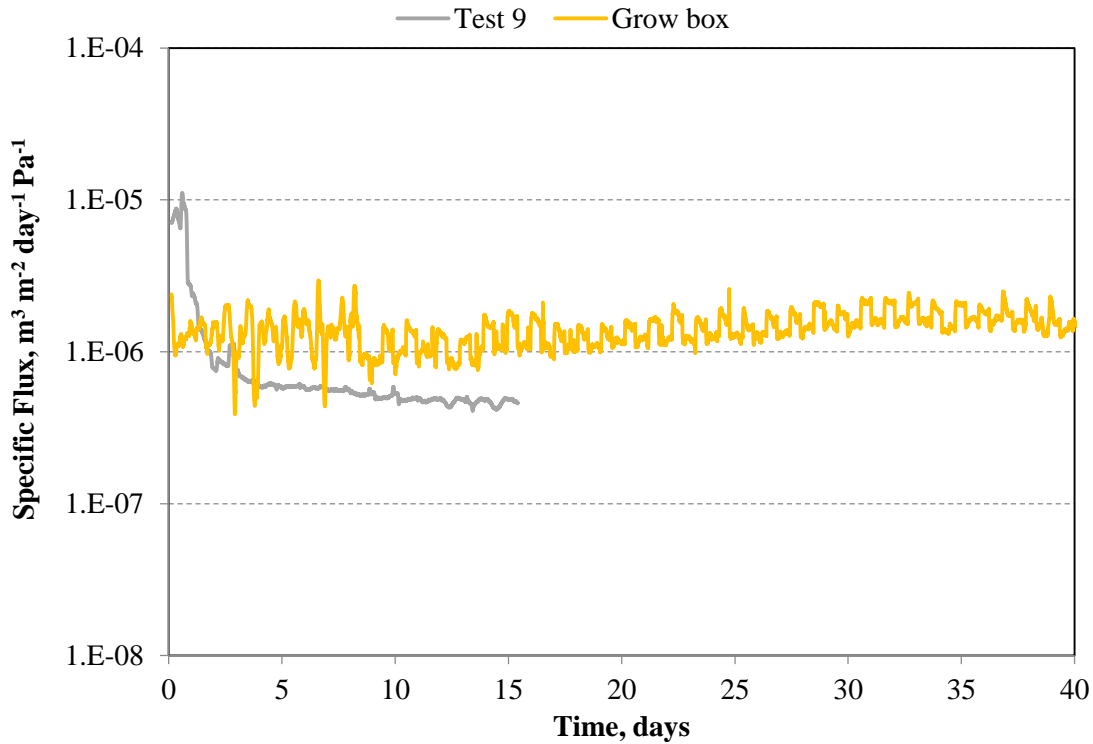


Figure 19 - Specific water flux through tubular CTA and PEE (Test 9) membranes. The PEE membrane (grey line) was surrounded by clay loam soil. The CTA membrane was surrounded by garden soil.



Figure 20 - Grow box snapshots. The snapshot at the top was taken at the beginning of the test (07/25/13) and the bottom picture was taken after approximately 140 days (12/16/13) after the start of the test. The plants which died were about 10 or more inches away from the center of the tube while the plants that were still alive at the end of test were inline or less than 5 inches away from the center of the PV tube.

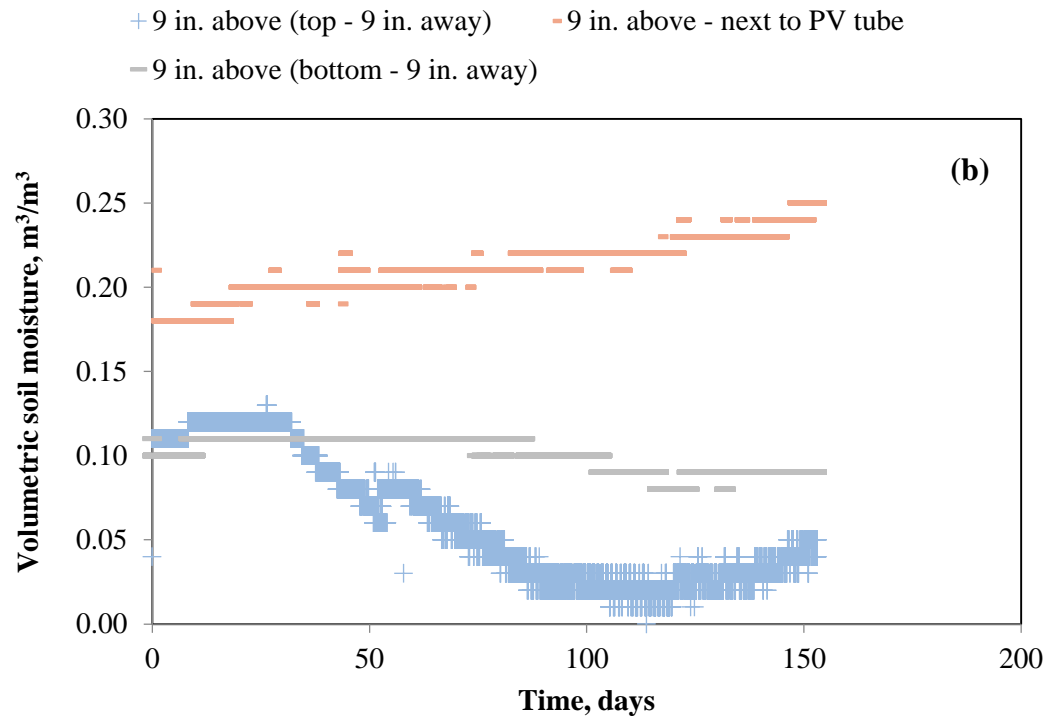
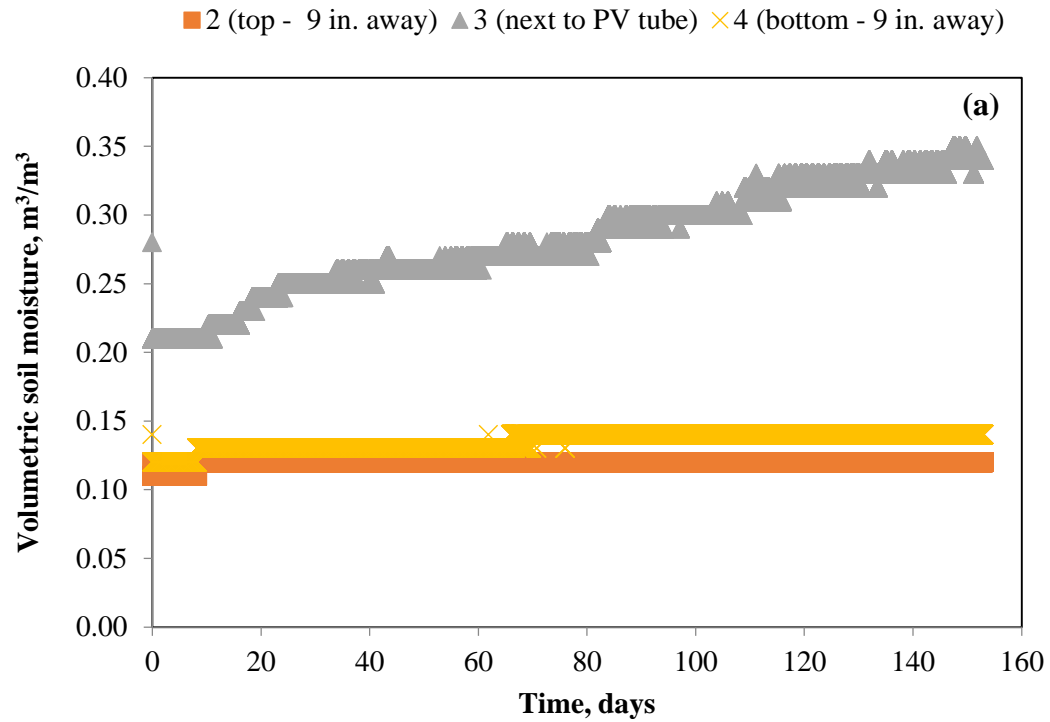


Figure 21 – Spatial variation in the grow box soil volumetric moisture content over the entirety of the grow box test.

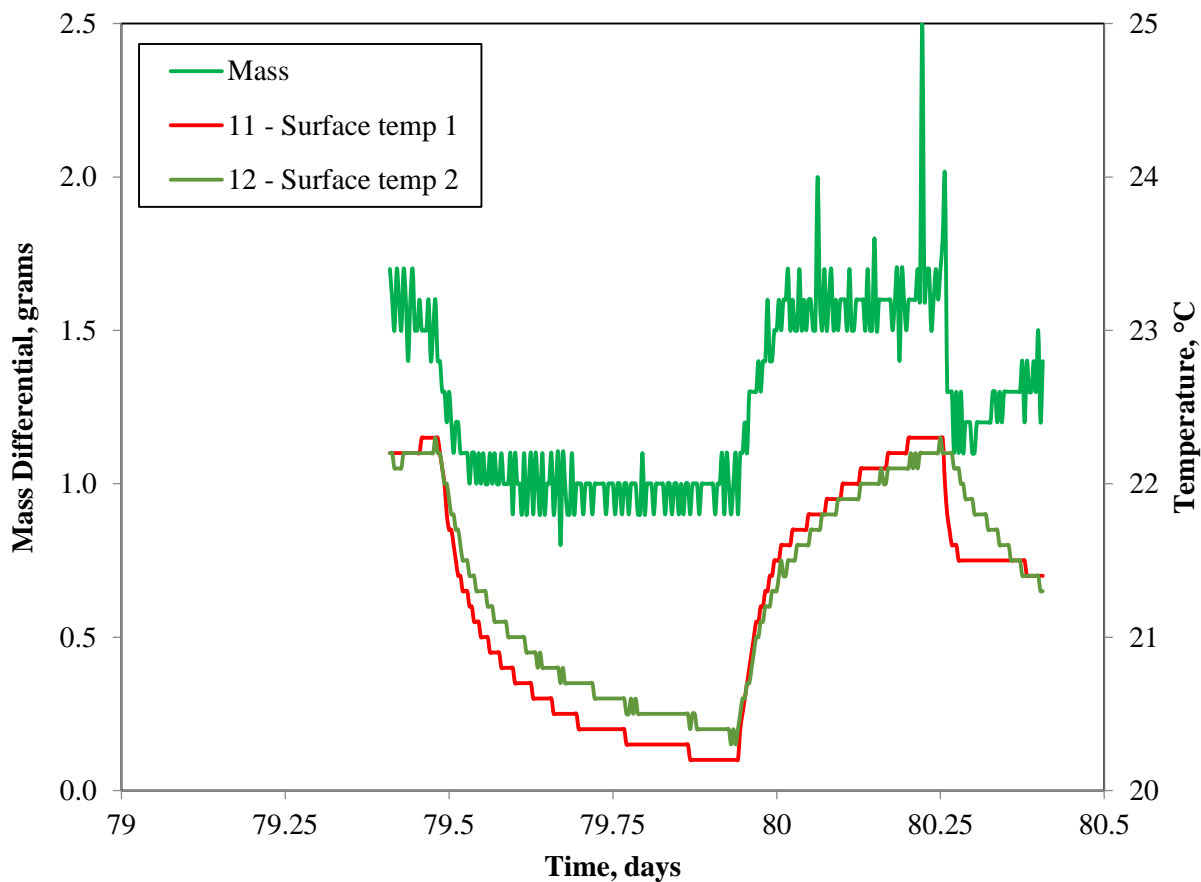


Figure 22 – Diurnal variation in the water flux across the CTA pervaporation membrane measured during the grow box experiment. Alfalfa was grown in the grow box during this test.

The variation of the pervaporation flux rate in a single day can be seen in **Figure 22**. The diurnal variation in the permeate flux rate across the pervaporation tube is due to the grow lights working on a day – night basis. The higher temperatures during the day contribute to a higher flux rate when compared to the night. The temperature within the soil surface as measured by the soil probes is plotted on the secondary y-axis. We see that it mirrors the trend in the mass loss as recorded by the feed weigh scale (corresponds to permeation flux).

Field-trial assessment of pervaporation irrigation

The results from the field trials are summarized in **Figure 23**. During the first two weeks the permeate flux was initially higher (5 - 9 kg/m²/day) than the average flux that was measured at $t \geq 3$ weeks. This trend is similar to that seen in the soil box experiments where the flux decreased

from an initially high value over the initial 24 hrs as a result of water adsorption by the membrane material. However, a distinction between the two types of tests is the amount of time that was required by the membranes to reach the plateau in the field trials (3 weeks versus 1 day). Also, the soil was very dry the week before and hence the vapor pressure gradient was very high. After 3 weeks the water flux maintained a relatively stable value of 3 kg/m²/day. Fluctuations in the measured flux can be partially explained when we look at the weekly cumulative rainfall. The flux decreased from week 2 to week 3. This can be attributed to the fact that the weekly cumulative rainfall during week 2 and week 3 was about 2 mm and 15 mm, respectively. The soil was wetter during week 3 during the higher rainfall and hence the ΔVP was lower resulting in the lower flux. Similarly the flux during week 4 was slightly higher than the flux during week 3 owing to rainfall of only 1 mm for the entire week.

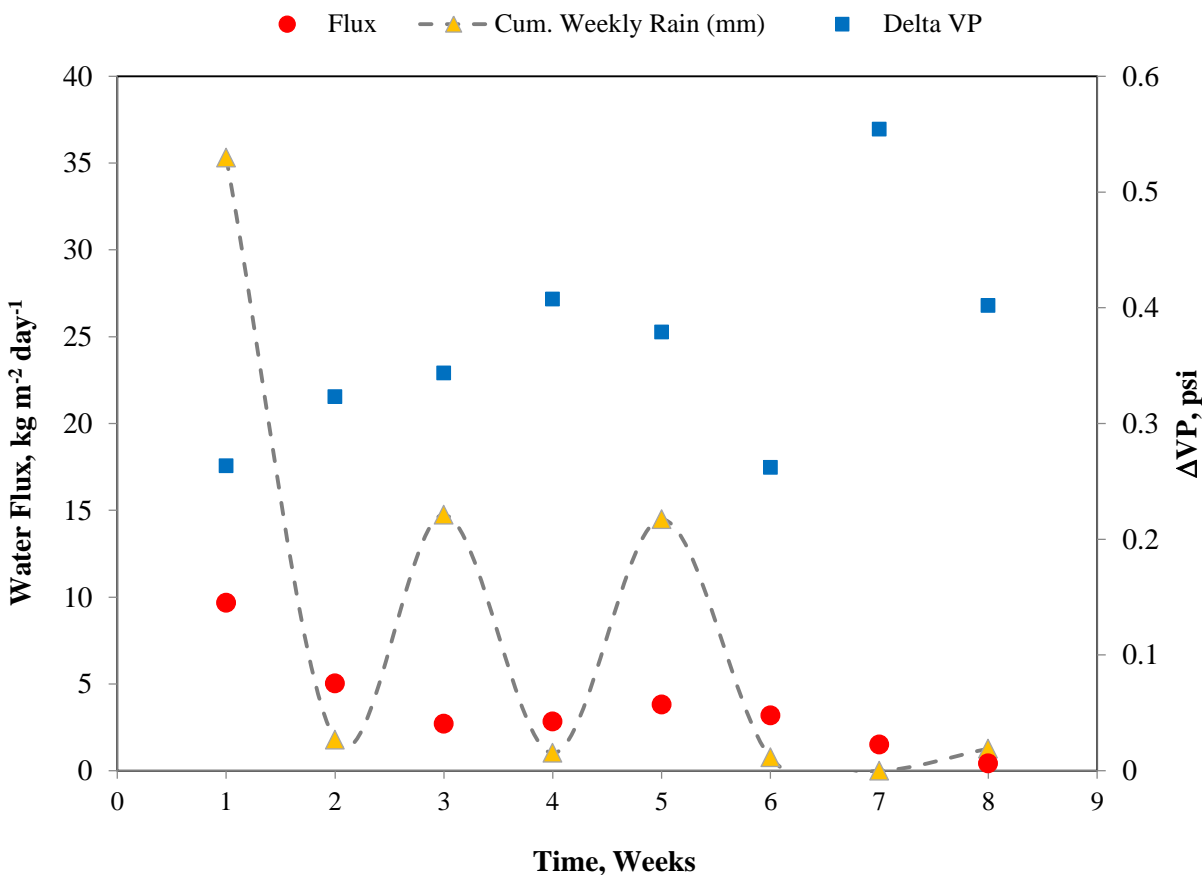


Figure 23 - Water flux (kg m⁻² day⁻¹), cumulative weekly precipitation (mm), and vapor pressure gradient for the tubular PEE membrane during field trials when treating CBM produced water.

PRACTICAL ASPECTS OF PERVAPORATION IRRIGATION

The practical application of pervaporation irrigation as a produced water management approach requires the consideration of the following variables:

- Land availability. Sufficient land must be available onto which the subsurface irrigation may be installed. Land area requirements will be a function of the volume of water to be disposed of, climate, and the type of crop(s) being irrigated. The principle characteristic of the impacted crop(s) is water uptake.
- Daily disposal volumes. While an effective desalination technique the water flux through the pervaporation irrigation tubes is small in comparison to existing membrane technologies. Therefore, this process is not well-suited for the disposal of relatively large volumes of water on a daily basis. The relative term “large” will be a function of different variables including crop characteristics, land area, climate amongst other considerations.
- Climate. Subsurface pervaporation irrigation is best suited for arid or semi-arid climates. In these environments the irrigated soils will maintain a relatively low soil moisture content which will maximize the water flux across the pervaporation membrane. Additionally, such environments will minimize risks associated with the tubes being installed in saturated soils. Saturated soil conditions may result in movement of water from the soil into the pervaporation tube through osmosis.
- Soil type(s) and groundwater elevation. The type of soil(s), and specifically the interaction between the soil and water, impacts the water flux across the membrane. Therefore, the soil type may be optimized for maximizing water flux in these systems; however, it is not a go/no go consideration for application of the subsurface pervaporation irrigation process. The maximum groundwater elevation must be below the bottom elevation of the irrigation network. This is required to prevent groundwater infiltration into the pervaporation tubes.
- Government regulations and public perception. As with any new technology implementation of the irrigation technology will require that all relevant regulations be met. Additionally, users must gain acceptance of the technology by all stake holders including participating farmers and ranchers.

The development of pervaporation membranes for subsurface irrigation applications is still in its infancy. Therefore, it is difficult to forecast the life expectancy of the tubes once they are buried in a given soil and under different climatic conditions. However, it is expected that the membranes will have a design life of no less than 5-yrs, which is comparable to that for conventional subsurface drip irrigation tubing. Such a life expectancy is needed to control capital and installation costs with subsurface pervaporation irrigation. The following is a non-exhaustive list of cost items in addition to those that will be incurred through acquisition of the pervaporation membranes themselves:

- Installation of the pervaporation tubes into the subsurface. This cost is expected to be comparable to that for the installation of conventional subsurface irrigation tape. The tubes will be designed so that they may be installed using the same, or slightly modified, equipment as that used in conventional subsurface irrigation applications.
- Produced water pretreatment. Although the pervaporation membranes have displayed a high tolerance for fouling the produced water may require pretreatment prior to use in the irrigation network. This need will be a strict function of the produced water composition and chemistry. For example, it may be necessary to adjust the solution pH to between 4 and 6 in order to minimize mineral scale formation and to meet the pH tolerance limits of the membrane material. Other treatments may focus on the removal of oils and greases, as well as aggressive solvents from the water in order to prevent plugging of the tubes and damage to the membrane materials.
- Water storage tanks and recirculation pumping. Storage will be required for the raw produced water that will be fed into the irrigation network as well as for the flush water that will be removed from the irrigation network on some predetermined schedule. A tank per se will not necessarily be required; however, sufficient head will be needed to feed the irrigation lines. A recirculation pump, which can also serve as a flush pump, will be needed to maintain a minimum scouring velocity in the irrigation lines. This will assist in mitigating fouling of the pervaporation membranes. Depending on the composition of the produced water the irrigation lines will require flushing using the raw produced water in order to remove those materials that accumulate within the irrigation lines as water permeates into the surrounding soil structure.

- Environmental monitoring. Because the source water to be used is classified as an industrial wastewater system monitoring will be required. Minimum monitoring requirements will likely include: leak detection for the storage device(s) and throughout the irrigation network, feed water quality (pH, conductivity/TDS), and soil characteristics (pH, conductivity).

IMPACT TO SMALL PRODUCERS

Findings from this project indicate that pervaporation irrigation is a viable alternative for disposing of, and reusing, produced waters. The treatment technology is best suited for managing low volumes of produced water and in locations already suited for agricultural activities. Of note is that use of the technology does not require that crops be grown. Indeed the technology may be employed for irrigating green spaces (natural grasses) or other areas requiring watering. The results gathered from the bench scale testing along with the grow box and field tests were used to construct the pervaporation irrigation modeling tool which would help small producers determine membrane requirements if they consider an irrigation based reuse strategy to treat produced water. Small producers can use the pervaporation treatment technology in existing field locations, since agricultural lands are often located close to them. Knowledge of some simple characteristics about the produced water, type of non-food crop selected, and some information regarding the size, location etc, of the plot is enough for small producers to make a decision on the feasibility of pervaporation irrigation as an environmentally friendly and cost effective disposal as well as reuse strategy. This reuse strategy will alleviate previous production and supply constraints that are related to process water availability and environmentally friendly produced water disposal.

TECHNOLOGY TRANSFER EFFORTS

We have presented findings from our work at a variety of professional conferences and in the form of two peer-reviewed publications. A list of the relevant conferences and publications is given below.

- Ruff, L. and **Brant, J.A.**, Pervaporation Desalination of High Salinity Oil and Gas Produced Waters, 2014 Membrane Technology Conference and Exposition, Las Vegas, NV, March 10-13, 2014.

- Brant, J.A., Treatment and Beneficial Reuse of Produced Waters using a Novel Pervaporation-Based Irrigation Technology, RPSEA Onshore Production Conference, June 27, 2013, Wichita, KS.
- Muthu, S., Huth, E., and Brant, J.A., Treatment and Reuse of Coal Bed Methane Produced Water Using Pervaporation Irrigation, RMWEA/RMSAWWA Student Conference, May 14, 2013, Golden, CO.
- Muthu, S., Huth, E., and Brant, J.A., Treatment and Reuse of Coal Bed Methane Produced Water Using Pervaporation Irrigation, Wyoming Groundskeepers and Growers Association Conference, February 14, 2013, Casper, WY.
- Brant, J.A., Treatment and Beneficial Reuse of Produced Waters using a Novel Pervaporation-Based Irrigation Technology, RPSEA Onshore Production Conference, November 29, 2012, Houston, TX.
- Huth, E. and **Brant, J.A.**, Treatment and Reuse of Coalbed Methane Produced Water Using a Pervaporation Irrigation Membrane Process, 22nd Annual Produced Water Society Conference, January 17-19, 2012, Houston, TX.
- Brant, J.A., Treatment and Beneficial Reuse of Produced Waters using a Novel Pervaporation-Based Irrigation Technology, RPSEA Onshore Production Conference, April 10, 2012, Midland, TX.
- Huth, E., and Brant, J.A., Treatment and Beneficial Reuse of Produced Waters using Pervaporation Irrigation, 2012 RMWEA/RMSAWWA Student Conference, May 18, 2012, Fort Collins, CO.
- Huth, E., Muthu, S., **Ruff, L.**, Brant, J.A., Performance Evaluation of Two Pervaporation Membranes for Desalinating High Salinity Brines, Journal of Water Reuse and Desalination – *accepted*
- Sule, M., Jiang, J., Templeton, M., Huth, E., **Brant, J.A.**, and Bond, T., Salt Rejection and Water Flux through a Tubular Pervaporative Polymer Membrane Designed for Irrigation Applications, Environmental Technology, Vol. 34 (10), 2013, 1329-1339.

CONCLUSIONS

1. Nonporous, hydrophilic pervaporation membranes were examined to determine its feasibility in beneficially treating and reusing produced water for irrigating crops.
2. The membrane performance (flux rate and rejection) was found to be highly dependent on the following parameters: membrane thickness (l), vapor pressure gradient (ΔVP , manipulated by changing the feed water temperature); affinity of water to the hydrophilic membranes; and feed water salinity. Water flux rates through flat-sheet PEE membrane samples were found to increase by upto 140% when the membrane thickness was decreased from 250 to 20 μm and the flux rates increased by as much as 50% when the ΔVP (temperature) was increased from 2295 up to 12275 Pa. An increase in salinity of the feed water was found to decrease the flux rates through the examined membranes (upto 800%). Both the polyetherester and cellulose triacetate membranes displayed excellent salt rejection capabilities (rejection $\geq 99\%$).
3. Performance (flux and rejection) of the tubular versions of the pervaporation membrane were also examined in an experimental setup which imitated an irrigation system, in which the tubing was buried in soil and water (vapor) was filtered through the tubing into the surrounding soil media. The tubular pervaporation membranes were found to show consistent permeate flux rates regardless of feed water salinity, and soil type surrounding the tubing.; although permeate flux rates were found to generally increase as the relative humidity and surrounding soil moisture decreased. Salt concentrations were found to increase during membrane operation, indicating good salt rejection capabilities and the potential for long term use as an irrigation system buried in the soil (because flux did not decline as the feed water quality decreased and even when precipitation was occurring inside the membrane tubing).
4. Overall, the nonporous hydrophilic pervaporation membranes examined showed potential to be used as a produced water treatment and irrigation system. However, when examining the membrane performance from an environmental engineering perspective rather than an agricultural perspective (in other words, using the membrane to treat the amount of water produced by the CBM well as opposed to the

amount of water needed to sufficiently supply a crop) several improvements would need to be made to the membrane material. In order to decrease the amount of surface area of tubing required to treat the water produced by a CBM well, it would likely be necessary to use a thinner membrane material. It would be best if the membrane thickness used in the field was thin enough (say $l \leq 100 \mu\text{m}$) to prevent the sharp decrease in membrane performance. It would also be best if the membrane chemistry could be manipulated (say through charge interactions) so that the membrane displayed more inherent rejection capabilities. It would be best to develop a membrane that would not fail (achieve breakthrough) if a flood event occurred which could potentially cause saturated conditions surrounding and complete passage of salts through the membrane.

RECOMMENDATIONS

Nonporous, hydrophilic pervaporation membranes did display potential for use as a produced water treatment and irrigation process, but there were found to be a few areas where development would be recommended.

1. The pervaporation membrane performance could be improved by developing a membrane with a smaller thickness which is still durable enough to be placed in the ground without the membrane being punctured by soil/organic matter. Properties desired would be better flux, higher rejection and good mechanical strength.
2. More work examining the role that the environment, soil and vegetation play on the pervaporation membrane performance is needed (more elaborate and longer pilot scale experiments in the field). Examining soils of different moisture content would be beneficial to examine how the change in water content in the soil affects the driving force for the pervaporation process. It would also be beneficial to examine how the presence of plants impacts membrane performance; it is expected that plants would act as a water sink and aid in transporting water vapor away from the permeate side of the membrane. More research should also be performed to determine the impacts the treated water can have on the surrounding soil and plant health. It is likely that some salts (particularly Na^+) can pass through the membrane, so it would be important to determine if the soil structure, water infiltration rates, and/or vegetation yield changed over time due to salts making it through the membrane.

REFERENCES

- [1] J.A.V.a.e. al., A White Paper Describing Produced Water from Production of Crude Oil, Natural Gas, and Coal Bed Methane, (2004).
- [2] J.A. Veil, C.E. Clark, Produced-Water-Volume Estimates and Management Practices, *Spe Prod Oper*, 26 (2011) 234-239.
- [3] K.L. Benko, J.E. Drewes, Produced Water in the Western United States: Geographical Distribution, Occurrence, and Composition, *Environmental Engineering Science*, 25 (2008) 239-246.
- [4] U.S.D.o.t. Interior, Oil and Gas Produced Water Management and Beneficial Use in the Western United States, (2011).
- [5] R.P. 07122-12, Technical Assessment of Produced Water Treatment Technologies, (2009).
- [6] L. ALL Consulting, Technical Summary of Oil & Gas Produced Water Treatment Technologies, (2005).
- [7] A. Fakhru'l-Razi, A. Pendashteh, L.C. Abdullah, D.R. Biak, S.S. Madaeni, Z.Z. Abidin, Review of technologies for oil and gas produced water treatment, *J Hazard Mater*, 170 (2009) 530-551.
- [8] E.T. Igundu, G.Z. Chen, Produced water treatment technologies, *International Journal of Low-Carbon Technologies*, (2012).
- [9] R. Mastouri, A Time to Review the Produced Water Treatment Technologies, A Time to Look Forward for New Management Policies, (2010).
- [10] M. Ahmed, W.H. Shayya, D. Hoey, A. Mahendran, R. Morris, J. Al-Handaly, Use of evaporation ponds for brine disposal in desalination plants, *Desalination*, 130 (2000) 155-168.
- [11] R. Shpiner, G. Liu, D.C. Stuckey, Treatment of oilfield produced water by waste stabilization ponds: Biodegradation of petroleum-derived materials, *Bioresource Technol*, 100 (2009) 6229-6235.
- [12] R. Dennis, Ion exchange helps CBM producers handle water, *Oil Gas J*, 105 (2007) 41-43.
- [13] R. Does, A. Hussain, M. Katebah, S. Adham, Advanced Water Treatment Technologies for Produced Water, (2012) 102-109.
- [14] J.D. Pless, M.L.F. Philips, J.A. Voigt, D. Moore, M. Axness, J.L. Krumhansl, T.M. Nenoff, Desalination of brackish waters using ion-exchange media, *Ind Eng Chem Res*, 45 (2006) 4752-4756.

- [15] S. Mondal, C.L. Hsiao, S.R. Wickramasinghe, Nanofiltration/reverse osmosis for treatment of coproduced waters, *Environ Prog*, 27 (2008) 173-179.
- [16] S. Mondal, S.R. Wickramasinghe, Produced water treatment by nanofiltration and reverse osmosis membranes, *Journal of Membrane Science*, 322 (2008) 162-170.
- [17] H. Ozgun, M.E. Ersahin, S. Erdem, B. Atay, B. Kose, R. Kaya, M. Altinbas, S. Sayili, P. Hoshan, D. Atay, E. Eren, C. Kinaci, I. Koyuncu, Effects of the pre-treatment alternatives on the treatment of oil-gas field produced water by nanofiltration and reverse osmosis membranes, *J Chem Technol Biot*, 88 (2013) 1576-1583.
- [18] T.Y. Cath, A.E. Childress, M. Elimelech, Forward osmosis: Principles, applications, and recent developments, *Journal of Membrane Science*, 281 (2006) 70-87.
- [19] T.Y. Cath, Osmotically and thermally driven membrane processes for enhancement of water recovery in desalination processes, *Desalin Water Treat*, 15 (2010) 279-286.
- [20] S. Phuntsho, S. Hong, M. Elimelech, H.K. Shon, Forward osmosis desalination of brackish groundwater: Meeting water quality requirements for fertigation by integrating nanofiltration, *Journal of Membrane Science*, 436 (2013) 1-15.
- [21] R.L. McGinnis, N.T. Hancock, M.S. Nowosielski-Slepowron, G.D. McGurgan, Pilot demonstration of the NH.sub.3/CO.sub.2 forward osmosis desalination process on high salinity brines, *Desalination*, 312 (2013) 67.
- [22] C.R. Martinetti, A.E. Childress, T.Y. Cath, High recovery of concentrated RO brines using forward osmosis and membrane distillation, *Journal of Membrane Science*, 331 (2009) 31-39.
- [23] B.L. Pangarkar, M.G. Sane, M. Guddad, Reverse Osmosis and Membrane Distillation for Desalination of Groundwater: A Review, *ISRN Materials Science*, 2011 (2011) 1-9.
- [24] M. Gryta, M. Tomaszewska, K. Karakulski, Wastewater treatment by membrane distillation, *Desalination*, 198 (2006) 67-73.
- [25] J. Zhang, M. Duke, E. Ostarcevic, N. Dow, S. Gray, J.-d. Li, Performance of new generation membrane distillation membranes, *Water Science & Technology: Water Supply*, 9 (2009) 501-508.
- [26] K.W. Lawson, D.R. Lloyd, Membrane distillation, *Journal of Membrane Science*, 124 (1997) 1-25.
- [27] L. ALL Consulting, Handbook on Coal Bed Methane Produced Water: Management and Beneficial Reuse Alternatives, (2003).
- [28] J. Neel, P. Aptel, R. Clement, Basic Aspects of Pervaporation, *Desalination*, 53 (1985) 297-326.

- [29] P. Shao, R.Y.M. Huang, Polymeric membrane pervaporation, *Journal of Membrane Science*, 287 (2007) 162-179.
- [30] M. Elma, C. Yacou, D.K. Wang, S. Smart, J.C. Diniz da Costa, Microporous Silica Based Membranes for Desalination, *Water*, 4 (2012) 629-649.
- [31] C. Chang, M. Chang, Preparation of multi-layer silicone/PVDF composite membranes for pervaporation of ethanol aqueous solutions, *Journal of Membrane Science*, 238 (2004) 117-122.
- [32] R. Jiraratananon, A. Chanachai, R.Y.M. Huang, D. Uttapap, Pervaporation dehydration of ethanol-water mixtures with chitosan/hydroxyethylcellulose (CS/HEC) composite membranes I. Effect of operating conditions, *Journal of Membrane Science*, 195 (2002) 143-151.
- [33] I.T. Meireles, C. Brazinha, J.G. Crespo, I.M. Coelho, A new microbial polysaccharide membrane for ethanol dehydration by pervaporation, *Journal of Membrane Science*, 425-426 (2013) 227-234.
- [34] G.M. Shi, T.-S. Chung, Thin film composite membranes on ceramic for pervaporation dehydration of isopropanol, *Journal of Membrane Science*, 448 (2013) 34-43.
- [35] J. Wang, T. Tsuru, Cobalt-doped silica membranes for pervaporation dehydration of ethanol/water solutions, *Journal of Membrane Science*, 369 (2011) 13-19.
- [36] X.-S. Wang, Q.-F. An, Q. Zhao, K.-R. Lee, J.-W. Qian, C.-J. Gao, Homogenous polyelectrolyte complex membranes incorporated with strong ion-pairs with high pervaporation performance for dehydration of ethanol, *Journal of Membrane Science*, 435 (2013) 71-79.
- [37] N. Widjojo, T.-S. Chung, Pervaporation dehydration of C2–C4 alcohols by 6FDA-ODA-NDA/Ultem® dual-layer hollow fiber membranes with enhanced separation performance and swelling resistance, *Chem Eng J*, 155 (2009) 736-743.
- [38] J. Zuo, Y. Wang, S.P. Sun, T.-S. Chung, Molecular design of thin film composite (TFC) hollow fiber membranes for isopropanol dehydration via pervaporation, *Journal of Membrane Science*, 405-406 (2012) 123-133.
- [39] K. Konieczny, M. Bodzek, D. Panek, Removal of volatile compounds from the wastewaters by use of pervaporation, *Desalination*, 223 (2008) 344-348.
- [40] F. Lipnizki, R.W. Field, Integration of vacuum and sweep gas pervaporation to recover organic compounds from wastewater, *Separation and Purification Technology*, 22-3 (2001) 347-360.
- [41] D.L. Yang, S. Majumdar, S. Kovenklioglu, K.K. Sirkar, Hollow-Fiber Contained Liquid Membrane Pervaporation System for the Removal of Toxic Volatile Organics from Waste-Water, *Journal of Membrane Science*, 103 (1995) 195-210.

- [42] M. Drobek, C. Yacou, J. Motuzas, A. Julbe, L. Ding, J.C. Diniz da Costa, Long term pervaporation desalination of tubular MFI zeolite membranes, *Journal of Membrane Science*, 415-416 (2012) 816-823.
- [43] E. Korin, I. Ladizhensky, E. Korngold, Hydrophilic hollow fiber membranes for water desalination by the pervaporation method, *Chem Eng Process*, 35 (1996) 451-457.
- [44] E. Korngold, E. Korin, I. Ladizhensky, Water desalination by pervaporation with hollow fiber membranes, *Desalination*, 107 (1996) 121-129.
- [45] Y.P. Kuznetsov, E.V. Kruchinina, Y.G. Baklagina, A.K. Khripunov, O.A. Tulupova, Deep desalination of water by evaporation through polymeric membranes, *Russian Journal of Applied Chemistry*, 80 (2007) 790-798.
- [46] E. Quiñones-Bolaños, H. Zhou, R. Soundararajan, L. Otten, Water and solute transport in pervaporation hydrophilic membranes to reclaim contaminated water for micro-irrigation, *Journal of Membrane Science*, 252 (2005) 19-28.
- [47] E. Quinones-Bolanos, H.D. Zhou, Modeling water movement and flux from membrane pervaporation systems for wastewater microirrigation, *J Environ Eng-Asce*, 132 (2006) 1011-1018.
- [48] M. Sule, J. Jiang, M. Templeton, E. Huth, J. Brant, T. Bond, Salt rejection and water flux through a tubular pervaporative polymer membrane designed for irrigation applications, *Environ Technol*, 34 (2013) 1329-1339.
- [49] Z.L. Xie, M. Hoang, T. Duong, D. Ng, B. Dao, S. Gray, Sol-gel derived poly(vinyl alcohol)/maleic acid/silica hybrid membrane for desalination by pervaporation, *Journal of Membrane Science*, 383 (2011) 96-103.
- [50] H. Zwijnenberg, G. Koops, M. Wessling, Solar driven membrane pervaporation for desalination processes, *Journal of Membrane Science*, 250 (2005) 235-246.
- [51] E. Quinones-Bolanos, H.D. Zhou, G. Parkin, Membrane pervaporation for wastewater reuse in microirrigation, *J Environ Eng-Asce*, 131 (2005) 1633-1643.
- [52] R.Z. Asadi, F. Suja, F. Tarkian, F. Mashhoon, S. Rahimi, A.A. Jameh, Solar desalination of Gas Refinery wastewater using membrane distillation process, *Desalination*, 291 (2012) 56-64.
- [53] C.W.M. C.P. McArdle, R. Soundararajan, K.E. Stevens, Pervaporation; Precision Irrigation of Strawberries Using Moderate EC Water Sources.
- [54] L.C. Todman, A.M. Ireson, A.P. Butler, M.R. Templeton, Water Vapor Transport in Soils from a Pervaporative Irrigation System, *J Environ Eng*, 139 (2013) 1062-1069.
- [55] E.E. Quinones Bolanos, Membrane pervaporation to reuse contaminated water for microirrigation, in, 2005.

- [56] E. Quinones-Bolanos, H.D. Zhou, R. Soundararajan, L. Otten, Water and solute transport in pervaporation hydrophilic membranes to reclaim contaminated water for micro-irrigation, *Journal of Membrane Science*, 252 (2005) 19-28.
- [57] J.A. Brant, A.E. Childress, Assessing short-range membrane-colloid interactions using surface energetics, *Journal of Membrane Science*, 203 (2002) 257-273.
- [58] C.J. Vanoss, Acid-Base Interfacial Interactions in Aqueous-Media, *Colloid Surface A*, 78 (1993) 1-49.
- [59] A. United States. Environmental Protection, National primary drinking water standards, United States Environmental Protection Agency, Washington, D.C., 2003.
- [60] I. United States. Dept. of Energy. Office of Scientific and Technical, E. United States. Office of Fossil, L. Argonne National, Water management technologies used by Marcellus Shale Gas Producers, United States. Office of Fossil Energy, Washington, D.C, 2010.
- [61] S.P. Pinho, E.A. Macedo, Solubility of NaCl, NaBr, and KCl in water, methanol, ethanol, and their mixed solvents, *JOURNAL OF CHEMICAL AND ENGINEERING DATA*, 50 (2005) 29-32.
- [62] S.S. Sablani, M.F.A. Goosen, R. Al-Belushi, M. Wilf, Concentration polarization in ultrafiltration and reverse osmosis: a critical review, *Desalination*, 141 (2001) 269-289.
- [63] A. Saeed, R. Vuthaluru, Y.W. Yang, H.B. Vuthaluru, Effect of feed spacer arrangement on flow dynamics through spacer filled membranes, *Desalination*, 285 (2012) 163-169.
- [64] A. Shrivastava, S. Kumar, E.L. Cussler, Predicting the effect of membrane spacers on mass transfer, *Journal of Membrane Science*, 323 (2008) 247-256.
- [65] H. Mo, H.Y. Ng, An experimental study on the effect of spacer on concentration polarization in a long channel reverse osmosis membrane cell, *Water Sci Technol*, 61 (2010) 2035-2041.
- [66] G.K. Ganjgunte, G.F. Vance, L.A. King, Soil chemical changes resulting from irrigation with water co-produced with coalbed natural gas, *Journal of environmental quality*, 34 (2005) 2217.
- [67] G.K. Ganjgunte, L.A. King, G.F. Vance, Cumulative soil chemistry changes from land application of saline-sodic waters, *Journal of environmental quality*, 37 (2008) S128.
- [68] G.K. Ganjgunte, G.F. Vance, R.W. Gregory, M.A. Urynowicz, R.C. Surdam, Improving saline-sodic coalbed natural gas water quality using natural zeolites, *Journal of environmental quality*, 40 (2011) 57.